SECTION 6

R. F. SYSTEM

6.1. Introduction to the Synchrotron R.F. System

6.1.1. The energy necessary to raise the accepted protons from 15 MeV to 7 GeV will be provided by an accelerating voltage in a r.f. cavity mounted in a straight section. Protons will obtain an average increase in energy of 6 keV on each traversal of the cavity. The orbital frequency of the proton beam increases from 355 kc/s at injection to 2.02 Mc/s at an energy of 7 GeV. The r.f. frequency is four times the orbital frequency (harmonic number = 4) and a fraction of the injected protons will be trapped into four phase stable regions or bunches, each proton describing a synchrotron oscillation about the stable phase angle of the accelerating voltage. The harmonic number of 4 is a compromise figure involving the radial synchrotron oscillation amplitudes and the effect of the total energy spread in the oscillations on the trapping efficiency. Initially, the betatron and synchrotron oscillations of some of the protons will occupy the entire vacuum chamber. Although these oscillations will reduce in amplitude as acceleration proceeds, it is important that the mean radial position is held near the centre of the vacuum chamber (R_o), or at whatever controlled deviation may be required.

6.1.2. During acceleration the magnet guide field rises from 290 gauss to 14 kilogauss and the frequency of the r.f. voltage from 1.41 Mc/s to 8.1 Mc/s. To maintain the correct radial position the frequency must follow accurately a given function of the magnetic field. Because successful acceleration depends on limited coherent phase motion, it will also be necessary to control the phase of the beam relative to the phase of the accelerating voltage.

6.1.3. A simplified block diagram of the planned system is given in Fig 6.1(i). The system will have four main sections:-

(i) The high power r.f. equipment, providing the accelerating voltage.

(ii) The low power r.f. equipment, or primary frequency generator (P.F.G.), providing an accurate and controllable frequency source for the high power r.f. system.

(iii) The beam control system, providing a means of comparing the radial position and phase of the proton bunches with suitable reference values and of correcting any deviations via the P.F.G.

(iv) The beam diagnostic system, giving the dimensions, positions and movement of the beam in the vacuum chamber at all times from injection to full energy.

6.1.4. A considerable amount of work has proceeded both on the beam control and diagnostic systems but, for clarity and the presentation of a coherent story, it has been found convenient to defer the account of this work to the second part of this report where a description of the use of the systems during commissioning can be included. This account concentrates on the details of the low and high power r.f. systems and the accelerating cavity.

6.1.5. The high power r.f. equipment is situated in straight section 8 in the magnet ring (Fig. 6.3.9). A pair of transmitter triodes supply r.f. power to the accelerating cavity (Figs. 6.3.1(i) and (ii)). The cavity is loaded with ferrite to allow tuning

over the required frequency range. Power losses in the ferrite have a peak value of 42 kW and the load due to the proton beam rises to 1.6 kW per 10^{12} protons at 7 GeV. Two series gaps in the cavity each develop 6 kV peak r.f. voltage and at the normal magnet field rise rate of 20 kilogauss/s, the synchronous phase angle is 150°.

6.1.6. The power triodes are driven from a drive chain with an input of about 2 V r.m.s. at an impedance of 100Ω derived from the P.F.G. The cavity is tuned to the accelerating frequency by means of a bias winding around the ferrite carrying up to 900 A peak from a special bias power supply. There are two alternative bias supply systems available; one (thermionic) was developed during the early design stages, the second (using high power transistors) was developed later and will normally be used in the system since it has considerably greater frequency response. The amplitude of the accelerating voltage at the cavity gaps is controlled by means of an automatic level control (A.L.C.) loop by which the accelerating voltage is maintained equal to a voltage analogue of the rate of rise of the magnetic guide field ($\dot{B}$), thus keeping the synchronous phase angle constant.

6.1.7. The low power r.f. (P.F.G.) is situated in the Nimrod main control room. It supplies a low level c.w. signal of accurately controlled frequency to the drive chain.. Coarse control is arranged as follows:

(a) The magnet field rise rate ($\dot{B}$) is measured by a pick-up loop in the magnet field.

(b) The pick-up loop output is integrated (giving a voltage analogue to B) and used to control the bias current on the ferrite core of a r. f. oscillator coil. The relationship between the oscillator frequency and the bias current is arranged to be very close to the law relating orbital frequency and guide field.

Fine control is obtained by regulating the voltage across two variable capacity diodes in parallel with the oscillator tuned circuit. The oscillator output is fed through an amplifier and gate to the drive chain. The P.F.G. has a voltage function generator, the curve corrector, which can correct the oscillator frequency through several hundred kilocycles at fixed intervals of magnet field. Thus the frequency law and the radial position of the beam can be set to close limits. The frequency at injection is accurate to ± 300 c/s.

6.1.8. The P.F.G. is also a source of timing pulses for many other machine functions. The B and $\dot{B}$ signals generate these pulses which are thus related directly to the magnet field and hence to the proton energy in the machine. Time delayed pulses are also available for injector timing signals and for functions such as target programmes during magnet 'flat top'. The $\dot{B}$ signal is also available for controlling the cavity voltage via the A.L.C. loop of the drive chain.

6.1.9. Besides providing open loop control of the accelerator frequency, via the curve corrector, the P.F.G. will also be an essential part of the beam control system. The radial and vertical position of the beam will be measured by means of induction electrodes through which the protons circulate. The radial electrodes will be slit diagonally (Fig 6.5.2(ii)) so that the voltages induced on the two halves will be equal when the beam is at R_o. The sum of the two voltages will be a measure of beam intensity and their difference divided by their sum will give the radial position. The radial signal will be compared with a reference voltage, the error signal being fed (via a low pass network) to the variable capacity diodes in the P.F.G.

6.1.10. Phase Control will also be via the P.F.G. A beam phase detector will compare the phase of a signal induced on an induction electrode with the phase of the r.f. cavity voltage.

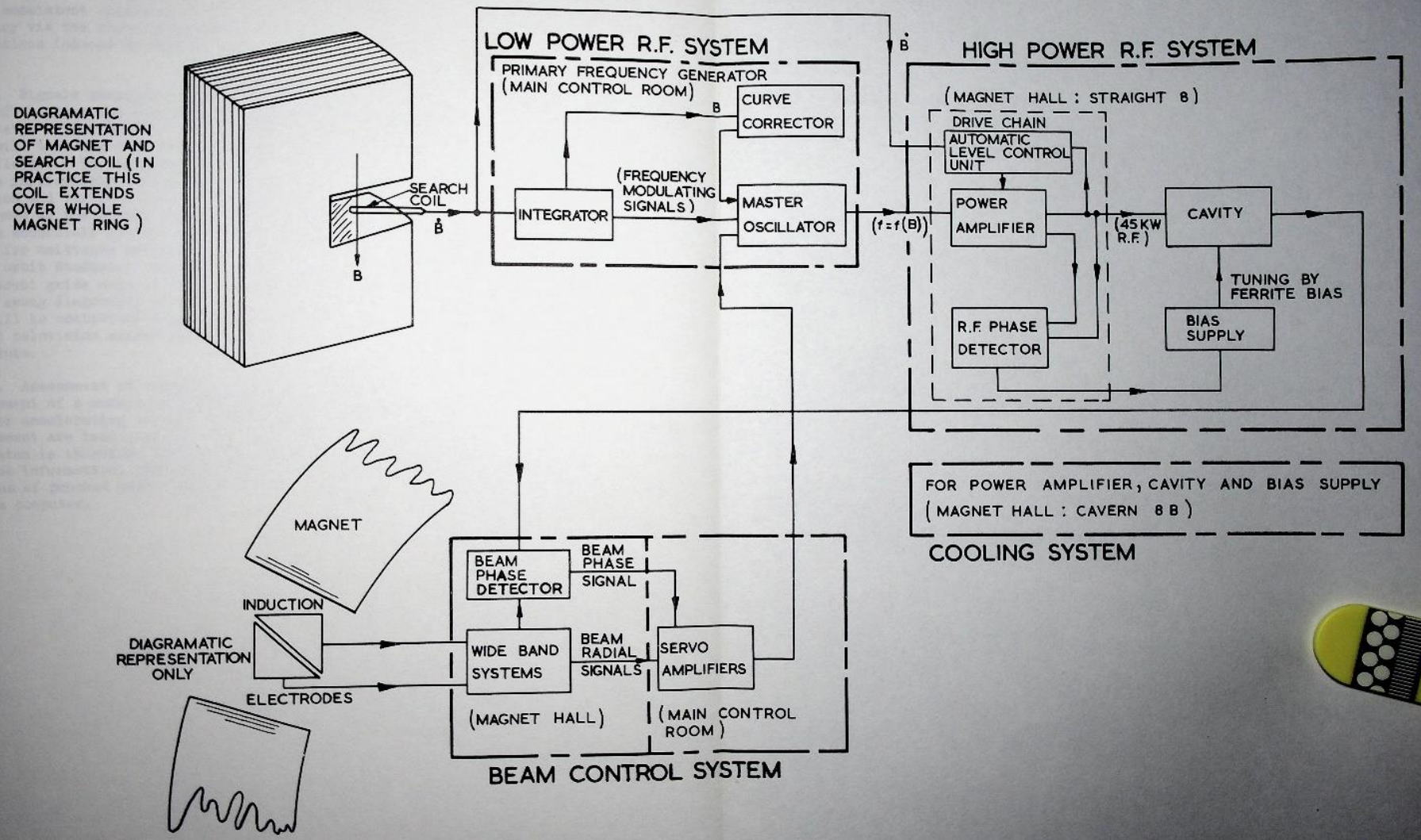

Figure 6.1(i) Simplified block diagram showing the principle of the planned r.f. accelerating system.

6.1.11. The two control loops will be gated independently. The radial loop should ensure consistent operation of the r.f. system without recourse to much adjustment of frequency via the curve corrector. The phase loop should damp coherent synchrotron oscillations induced by magnet ripple, and r.f. voltage and frequency errors.

6.1.12. Signals proportional to the magnitude, radial position, vertical position and phase of the beam are essential in tracing faults and adjusting many of the machine parameters. They will be used in combination with signals from diagnostic probes which will take the form of targets made of metal (for charge collection) or plastic scintillator. The induction electrode signals obtained with chopped injected beams will be particularly useful for the measurement of radial betatron oscillations during injection and vertical oscillations, if they exist. The diagnostic probes will be positioned at ten points around the machine (see part 2 of the Nimrod report). They will be accurately located by means of remotely controlled position servos. They will be useful for emittance and energy spectrum measurements on the injected beam and for closed orbit studies. For more direct observation of the beam, it is planned to use transparent grids made of fine wire coated with fluorescent material. These grids can be swung diagonally across the vacuum chamber behind windows in each octant. They will be controlled remotely and will be viewed through the windows by a closed circuit television system which will display all the grids simultaneously on a split field tube.

6.1.13. Assessment of changes in machine parameters may involve the simultaneous measurement of a number of quantities such as beam intensity, radial position, magnet field or accelerating voltage and frequency. The usual methods of oscilloscope measurement are inadequate in many instances for these requirements. A data recording system is therefore being developed which can handle six channels of voltage analogue information, each at a rate of 1000 readings/s. Read out will be either by means of punched paper tape which can be fed into a teleprinter or direct to an on-line computer.

6.2. Low Power R.F. System

6.2.1. Introduction

The purpose of the low power r.f. system (N.B. the "heart" of the system is often referred to as the primary frequency generator or P.F.G.) is to produce a r.f. voltage whose frequency is related to the guide field of the magnet as shown in Fig. 6.2.1(i).

The required performance can be considered under four headings:-

(a) Frequency stability at injection,

(b) Frequency tracking,

(c) Frequency stability at full energy and

(d) Frequency deviation noise.

The development took place in three stages: first, a system using thermionic valve circuitry throughout; second, a system using valves in the r.f. and d.c. amplifier circuits and transistors in the ancillary control circuits, and finally, using transistor circuitry throughout. Comparing the first and last systems, the volume has decreased from five racks of equipment to two, and the power consumption from over 1 kW to less than 90 W. Each stage of development improved the performance. The "perfect" switch action of transistors and the general lower impedance level resulted in circuits that were more stable and less sensitive to outside interference.

6.2.2. Description of System

A schematic diagram of the system is shown in Fig. 6.2.2(i).

A voltage proportional to the rate of rise of the magnet field is produced by a pick up loop in the magnet gap and this is integrated to produce a voltage proportional to the magnet guide field. The integrator is controlled by signals derived from the magnet power supply and from a peaking strip which determines the constant of integration.

The oscillator is a permeability tuned Colpitts oscillator, with a frequency range of 1.4 to 8 Mc/s, obtained by varying the incremental permeability of the ferrite inductance using a polarizing current of 4 A maximum. The output voltage of the integrator (30 V maximum) is converted into a current (4 A maximum) by means of the voltage to current converter.

The tracking law of frequency against magnetic field is chiefly derived from the design of the oscillator tank circuit and small deviations are corrected by means of an arbitrary function generator controlled by the magnet field. When the synchrotron is finally operational it is probable that this function generator will be replaced by a voltage derived from measurements of the radial beam position.

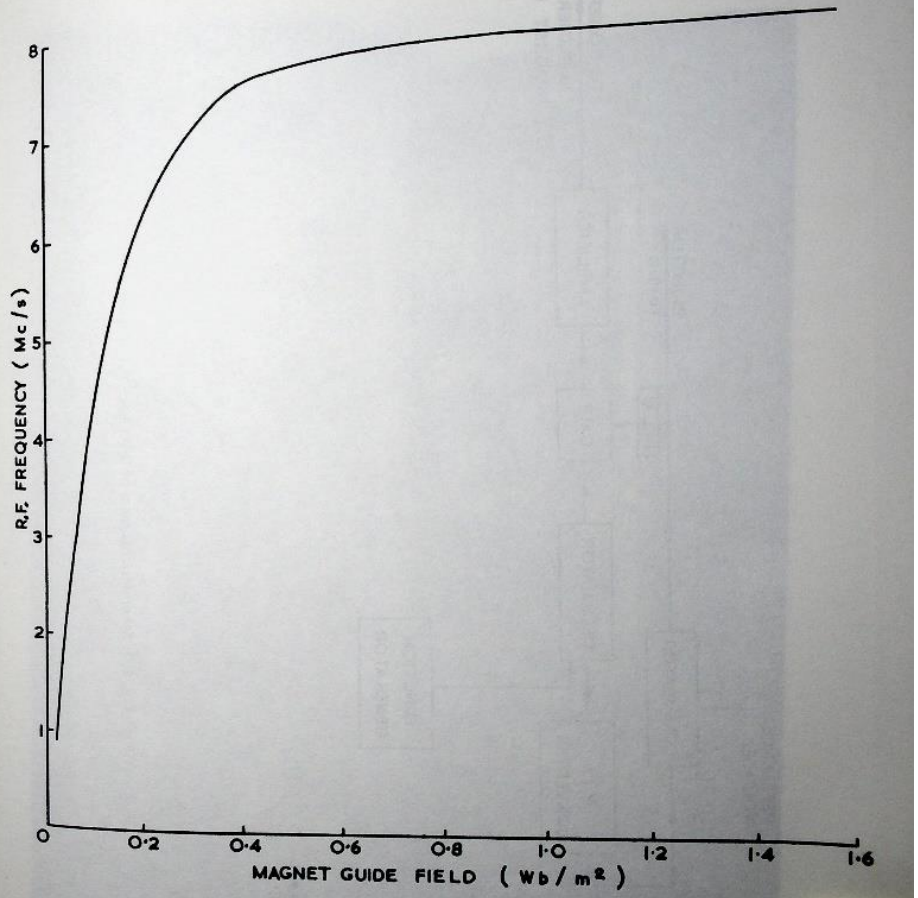

Fig. 6.2.1(i) Relationship of r.f. frequency to magnet guide field.

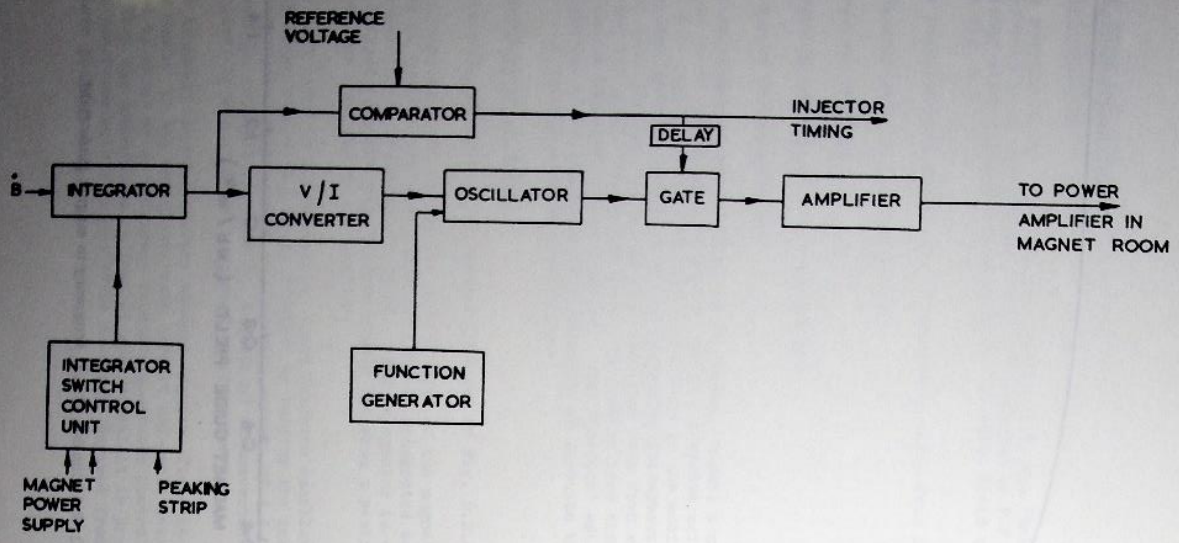

Fig. 6.2.2(i) Schematic diagram of low power r.f. system.

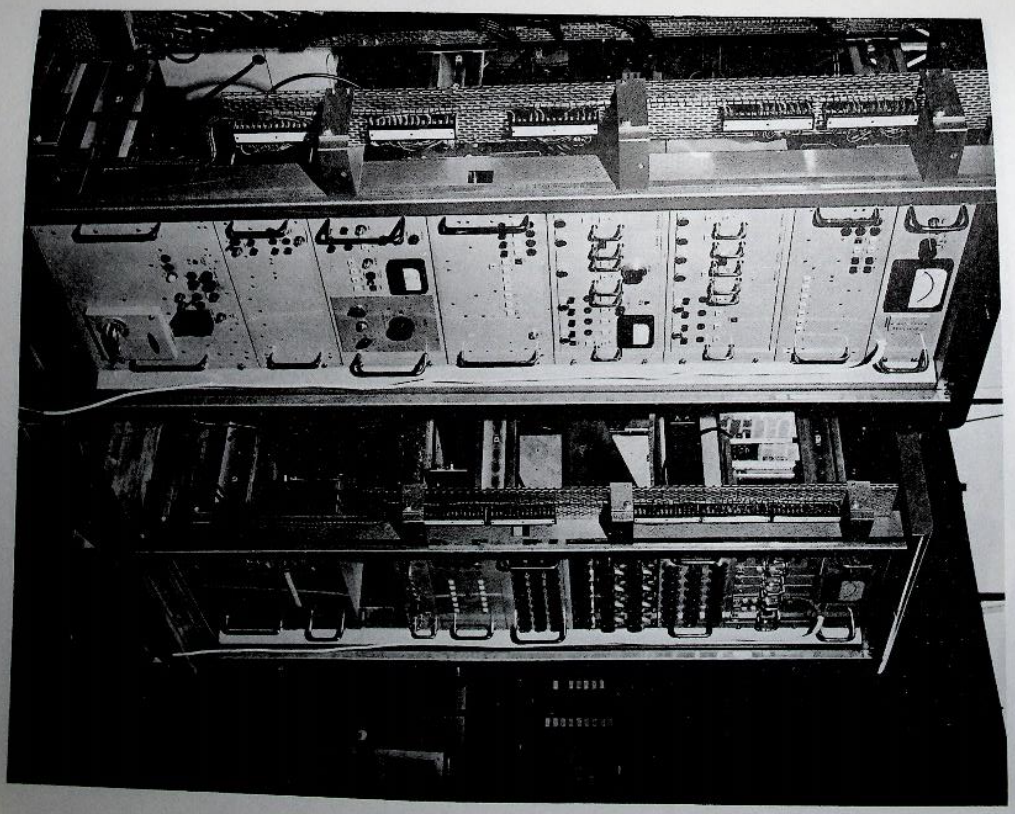

Fig. 6.2.3(i) Front view of low power r.f. units.

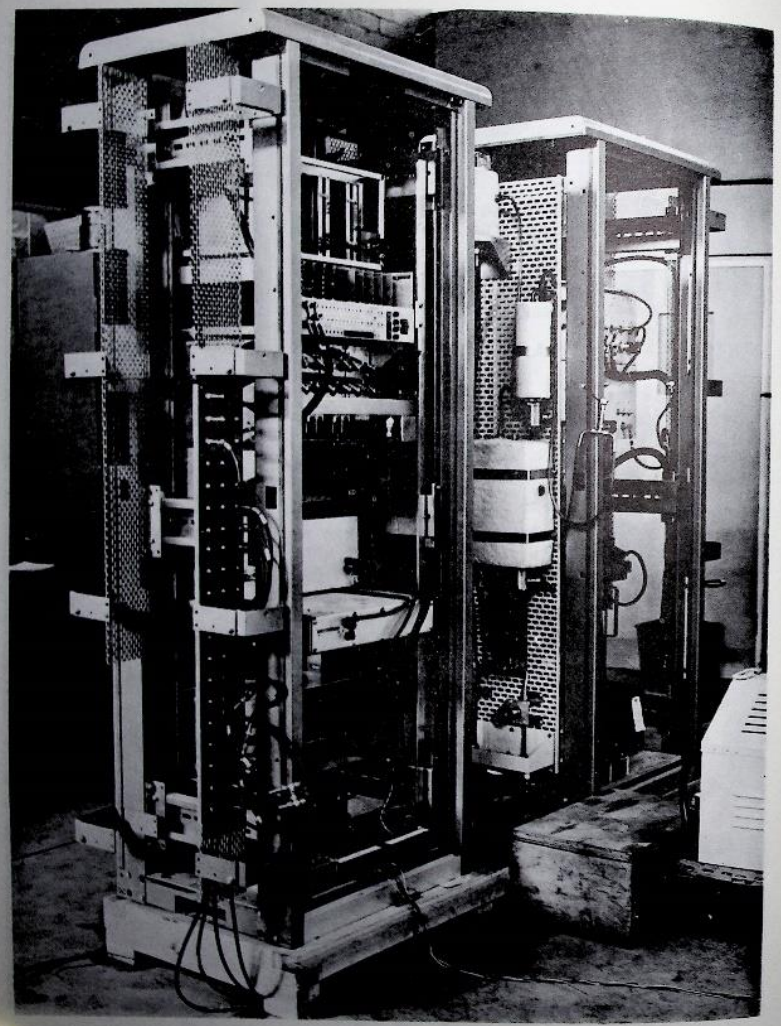

Fig. 6.2.3(ii) Rear view of low power r.f. units.

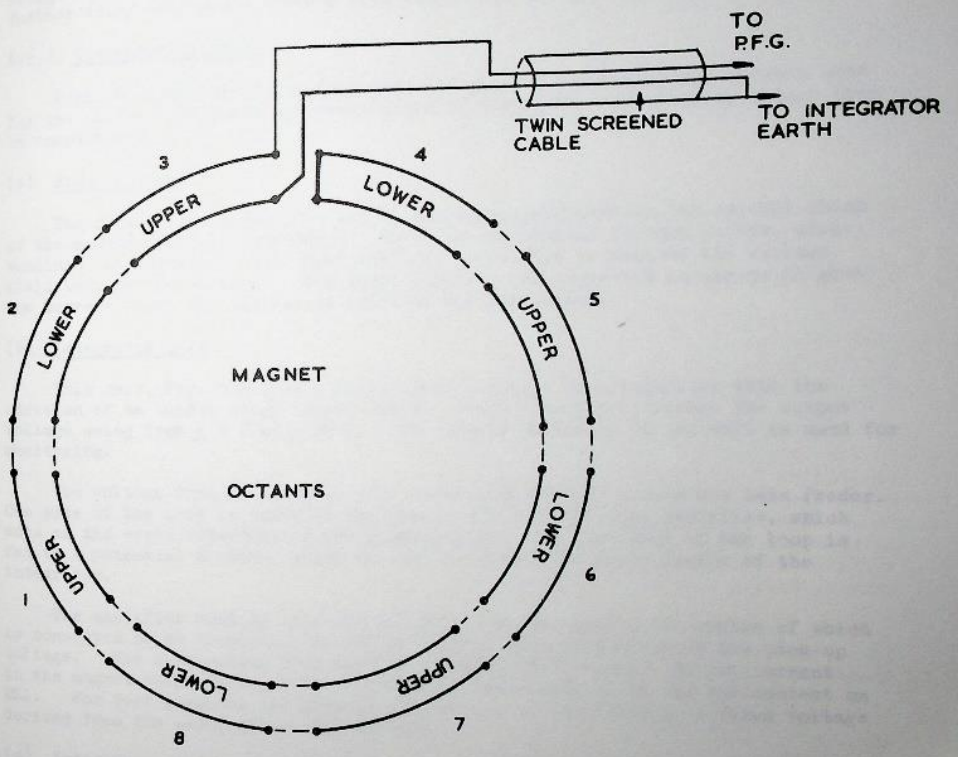

Fig. 6.2.3(iii) Schematic layout of pick up loop.

The peaking strip signal is obtained when the magnet field is approximately 160 gauss and the accelerating voltage has to be switched on at approximately 280 gauss. This delay is introduced by feeding the integrator output into a comparator, which produces an output pulse when the input voltage is equal to a reference voltage. This comparator could also be used for triggering the injector by an appropriate choice of reference voltage and a further delay introduced between this signal and the gate opening signal.

6.2.3. Component Circuits

Figs. 6.2.3(i) and 6.2.3.(ii) show the general constructional methods used for the units. Emphasis has been placed on "in situ" accessibility rather than on compactness.

(a) Pick up loop.

The pick up loop, Fig. 6.2.3(iii) encloses approximately the central third of the magnet aperture, radially There is one section in each octant, with windings alternately in the upper and lower pole face to measure the average field seen by the protons. The eight sections are connected in series to give the correct level for optimising drift in the integrator.

(b) Integrator unit

This unit, Fig. 6.2.3(iv), is designed around a d.c. amplifier with the addition of an output stage (shown inside dotted lines) to increase the output voltage swing from $\pm$ 6 V to $\pm$ 30 V. The second amplifier in the unit is used for monitoring.

The voltage from the pick-up loop enters the unit by a screened twin feeder. One side of the loop is taken to the signal earth of the d.c. amplifier, which acts as the earth reference of the pick-up loop; the live side of the loop is fed to a potential divider, which is used to adjust the scale factor of the integrator.

The amplifier summing resistor is split into two parts, the centre of which is connected to an electronic switch to control the application of the pick-up voltage. The integrating condenser is a plastic foil type. As the current in the magnet coils falls, this condenser is discharged by R1 and the contact on RL1. For test purposes the pick-up voltage can be simulated by a fixed voltage derived from the Zener diodes MR1 and MR2.

(c) Integrator switch control unit

The unit, Fig. 6.2.3(v), controls the integrator on receipt of three input pulses, P_1, P_2 and P_3. These are derived at the following times: P_1 - just before the magnet field starts to rise; P_2 - at a precise value of magnet field (approximately 160 gauss) just before the field corresponding to injection; P_3 - after acceleration, at the end of the magnet flat top. Pulses P_1 and P_3 are supplied by the magnet power supply control system and P_2 from a peaking strip.

There are two parts to the unit, the first, J1 to J4 controlling the relays RL1 (situated in the integrator unit) and RLC (situated in the V/I converter unit); the second, J5 to J8 controlling the clamp MR7-10, which is applied to the junction of the summing resistors in the integrator unit.

J2 and J3 form a conventional bistable circuit, the windings of the above relays forming the collector loads of J2 and J3. The circuit is set and reset by J1 and J4. A positive pulse P_3 applied to J4 closes the relay contact RL1-1 which discharges the integrating capacitor; it also operates the relay contacts RLC-1 to change from the forward to the reverse bias condition of the ferrite core of the oscillator tank inductance. A positive pulse P_1 applied to J1 reverses the action, allowing the integrator to operate and changing the reverse bias back to forward bias (via the V/I converter).

J6 and J7 form a complementary bistable circuit set and reset by J5 and J8. A positive pulse P_3 applied to the primary winding T_3 results in the transistors J6 and J7 being cut off. Current flows from the positive supply rail via R27 and R25 through the bridge MR7-10 and then via R16 and R15 to the negative supply rail. This results in the output point SK16 being clamped to earth. The potentiometer RV1 is adjusted to eliminate mismatch between the diodes.

A positive pulse P_2 applied to J5 causes the transistors J6 and J7 to saturate and reverse biases the bridge diodes and so unclamps the output point, allowing the voltage from the pick-up winding to be applied to the integrator.

(d) V/I converter

The output from the integrator approximates to a sawtooth with 28 V corresponding to 14 kilogauss. The frequency modulation characteristic of the oscillator is such that this has to be converted into a sawtooth of current, with 4 A corresponding to 14 kilogauss.

The unit (Fig. 6.2.3(vi)) is designed round the same d.c. amplifier as used in the integrator. The high voltage output stage is, in this case, followed by an emitter follower J5 driving a pair of transistors J6, J7 connected in parallel. Resistors R31-40 are used to improve load sharing between the transistors. The load, which is the polarizing winding on the oscillator tank inductance, is shown in dotted lines. The current through the load is monitored by the 4 Ω resistor (also shown dotted) and the voltage across this is fed back to produce a stable, linear transfer characteristic.

To compensate for a slight non linearity in the initial frequency modulation law of the oscillator, the transfer characteristic of this unit is modified by the diodes MR1 and MR2 and their associated components.

The reverse bias potentiometer is set for approximately 30 mA of reverse current in the polarizing winding of the oscillator tank inductance to cancel the polarized memory left by the 4 A forward saturation current of the ferrite, which would increase with successive cycles. The forward bias control is set so that the r.f. "start" frequency is correct at injection magnet field.

(e) Oscillator and gated amplifier

The oscillator unit (Fig. 6.2.3(vii)) contains the oscillator transistor J1 and most of the frequency determining elements, all mounted in a brass cylinder through which oil is circulated at a constant temperature. The oscillator circuit is a common collector Colpitts circuit with inductors L3 and L4 (in parallel) and capacitors C6 and C7 as the principle components. L3 and L4 are each wound on a separate ferrite toroid with a common polarizing winding L5. The two r.f. windings are connected so that no r.f. voltage is induced in the polarizing winding. The final frequency and the shape of the frequency modulation characteristic at the knee are determined by the inductance L6 and variable capacitor VC1.

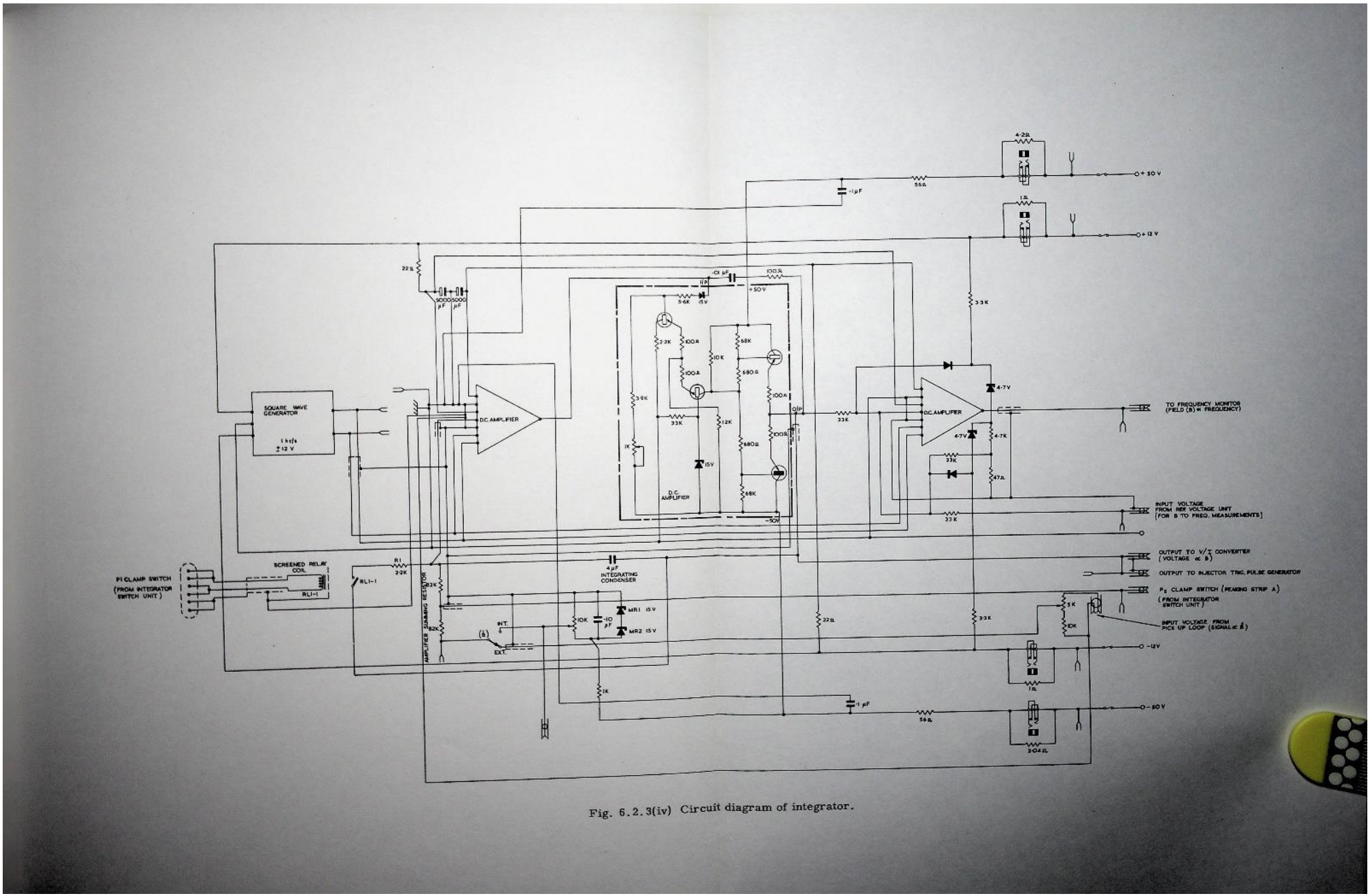

Fig. 6.2.3(iv) Circuit diagram of integrator.

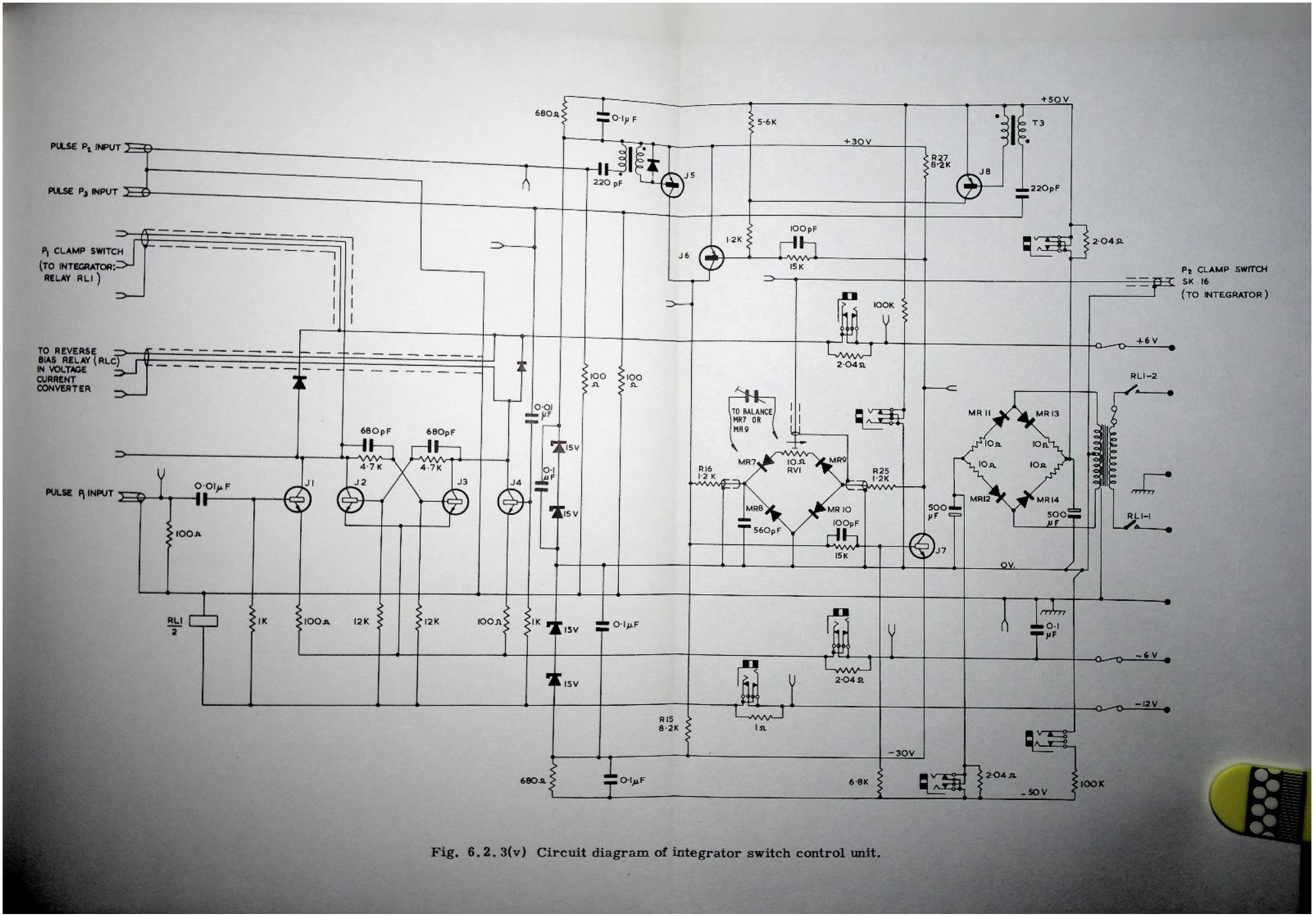

Fig. 6.2.3(v) Circuit diagram of integrator switch control unit.

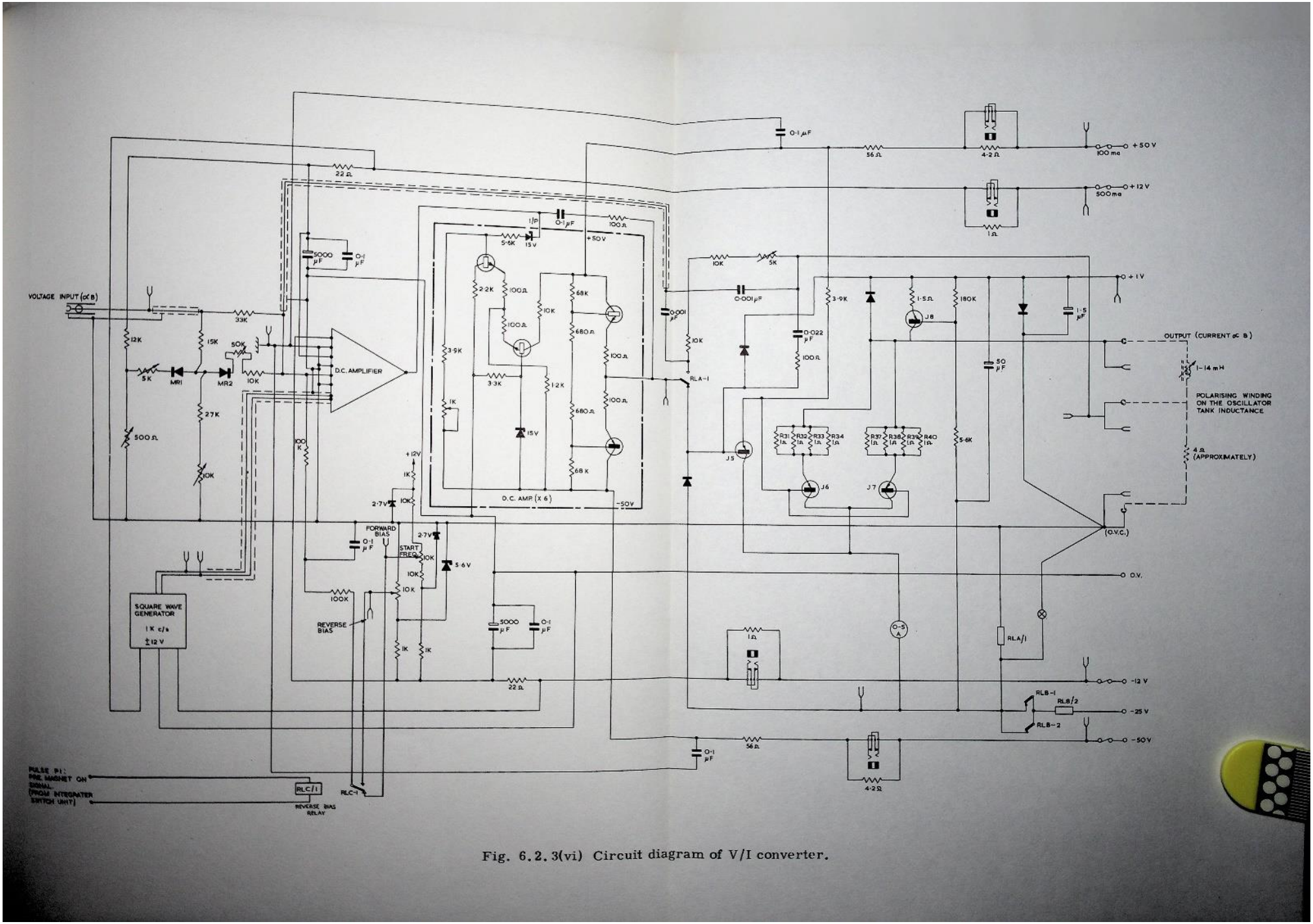

Fig. 6.2.3(vi) Circuit diagram of V/I converter.

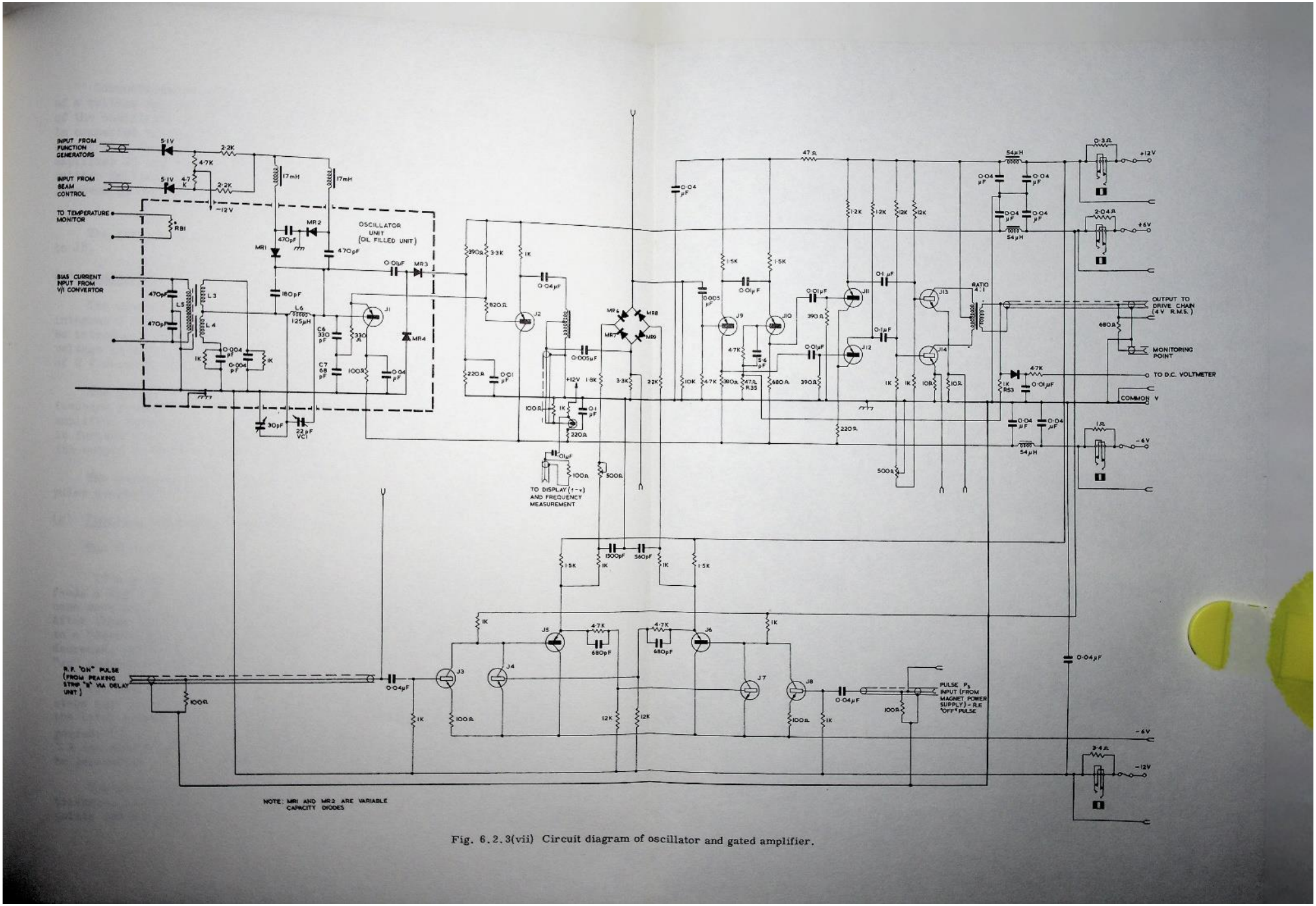

Fig. 6.2.3(vii) Circuit diagram of oscillator and gated amplifier.

Corrections to the frequency modulation characterstic are obtained by means of a voltage applied to the variable capacity diodes MR1 and MR2. The amplitude of the oscillator output is limited by the diodes MR3 and MR4. The oscillator is connected to the diode gate MR6 - 9 by the isolating emitter follower J2. The output from the gate is amplified and phase split by the emitter coupled amplifier J9 and J10 and applied to the output push pull pair J13 and J14 via emitter followers J11 and J12. The gain, stability and frequency response are improved by feedback via R53 and R35 to the base of J10.

The gate is controlled by the bistable circuit using transistors J3 to J8.

(f) Comparator

The comparator circuit is shown in Fig. 6.2.3(viii). The output from the integrator has a scale factor of 28 V representing 14 kilogauss. The delay to be introduced is approximately 100 gauss represented by 0.2 V. The integrator voltage is first amplified by a factor of 10 and then compared with a reference of 2 V derived from Zener diode MR6 and its associated potential divider.

The difference is amplified by the second d.c. amplifier which, having no feedback, produces a rapid transition from negative to positive saturation as the amplified integrator voltage passes through the reference voltage. The output is further sharpened by the complementary trigger circuit J1 and J2, and triggers the output blocking oscillator J3.

The performance of the comparator (also known as the injector trigger pulse generator) is described in detail elsewhere (5).

(g) Function generator (Curve corrector)

The function generator is discussed in general terms:

If a clock pulse train feeds an eight stage binary counter which (in turn) feeds a digital to analogue converter, then the first 256 pulses produce a staircase waveform with 256 steps at the output of the digital to analogue converter. After these 256 pulses, the counter is automatically changed from an "up" counter to a "down"counter, causing the output of the digital to analogue converter to decrease, again in 256 steps, to zero. The counter is then changed back to an "up" counter and the cycle repeated.

The resultant output waveform is marked (a) in Fig. 6.2.3(ix) where the steps are smoothed out. By taking outputs from both sides of the binary stages the interleaved waveform shown dotted is produced. The outputs during the periods T_1, T_2, T_3 etc. can each be independently adjusted to any value between $\pm A$ and therefore a function with the waveform marked (b) in Fig.6.2.3(ix), can be generated.

The advantage of this method of generating a function by a series of triangles rather than linear sloping segments, is that any one of the function points can be adjusted without having to alter any of the adjacent points.

The above description, indicates an operation which will produce an output as a function of time. It can be converted to a function of magnetic field, B, by replacing the clock train by a train of pulses, each pulse corresponding to an equal increment of B. This pulse train is obtained from B by using a digital integrator with an output pulse for every increment of 0.4 gauss.

With this system, each segment of the function generator corresponding to 256 clock pulses is 102.4 gauss and the 20 segments in the generator correspond to 2.05 kilogauss. This does not cover a sufficient fraction of the 14 kilogauss increase in magnetic field but the fine steps of 100 gauss are needed at the start.

These limitations are overcome by feeding the magnet ΔB train into two binary dividers B_1 and B_2, (Fig. 6.2.3(x)). The original input and the outputs from the two dividers are fed to gates G_1, G_2 and G_3, with a common output which is used as the new input train from the magnet.

Control waveforms are applied to the gates, such that G_1 is opened for say the first 6 segements, G_2 is opened for say the second 6 segments and G_3 is opened for the remaining segments. Under these conditions the interval for the first 6 segments will be 100 gauss, for the second 6 segments will be 200 gauss and for the last 7 will be 400 gauss.

6.2.4. Performance of System

Most attention is given to considerations of cycle to cycle jitter as this is much more troublesome than a gradual regular drift, which can be offset by an operator if the time between these adjustments is of the order of hours. A figure of 10% instability in beam current is regarded as an acceptable level.

Most of the measurements quoted have been taken under dynamic conditions corresponding to a standard machine pulse.

(a) Frequency stability at injection

At injection, when the aperture is "full" of particles, any frequency deviations will cause a loss of beam. It is uncertain at present, how the particles will be distributed in terms of betatron oscillation amplitude but a pessimistic assumption indicates that a 10% loss of particles will be produced by a frequency error of 0.05%. With a starting frequency of 1.43 Mc/s the tolerance is 715 c/s.

Since the "zero" of the system is determined by the peaking strip, errors in the peaking strip signal will be reflected as frequency errors. Assuming random errors equally distributed between the peaking strip and the low power r.f. system, the stabilities required are 0.1 gauss for the peaking strip and 500 c/s for the r.f. The frequency jitter corresponding to injection has been measured using simulated input signals and has a standard deviation of 360 c/s. This total has contributions from several sources and an attempt has been made to split the error into its various components.

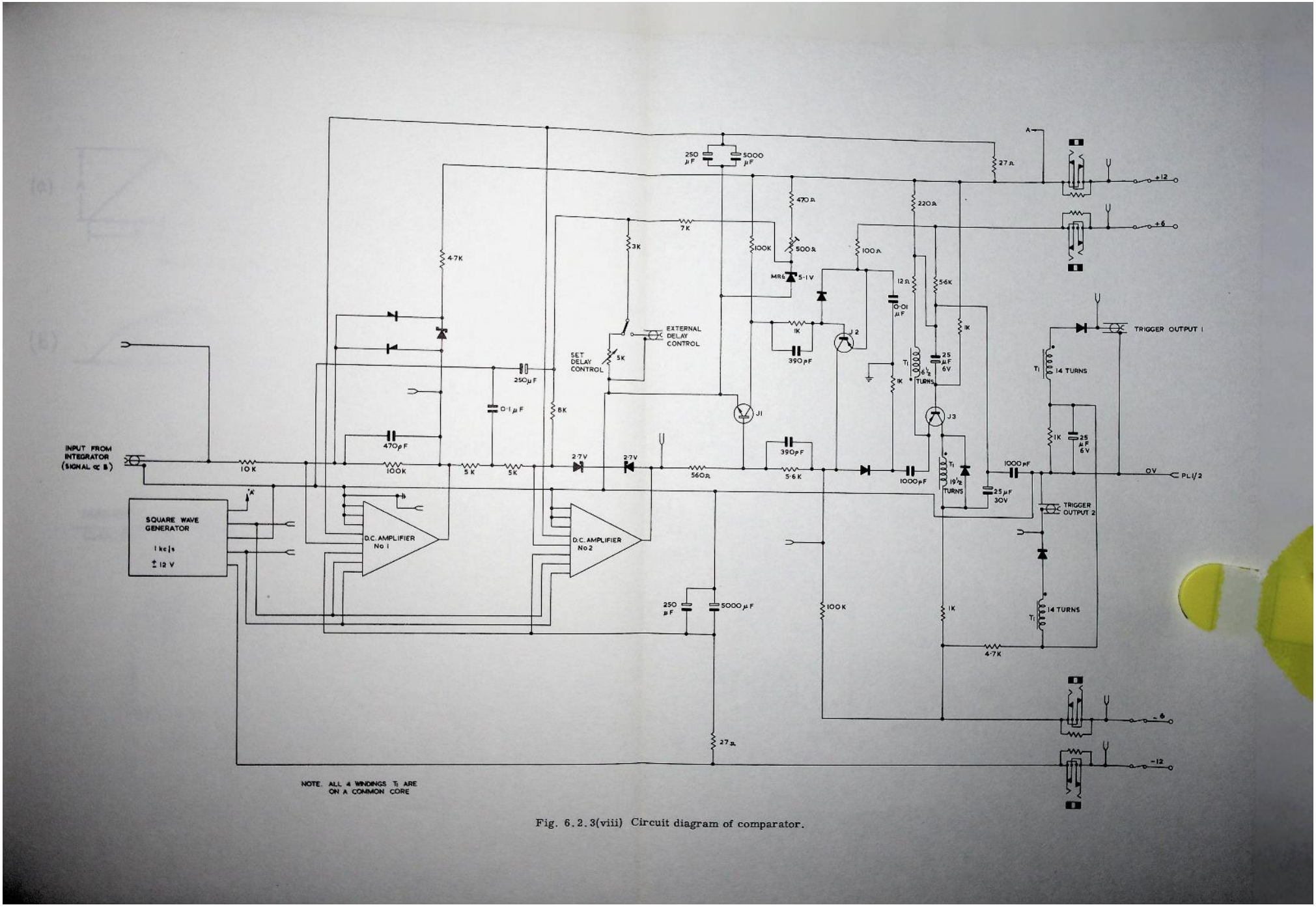

Fig. 6.2.3(viii) Circuit diagram of comparator.

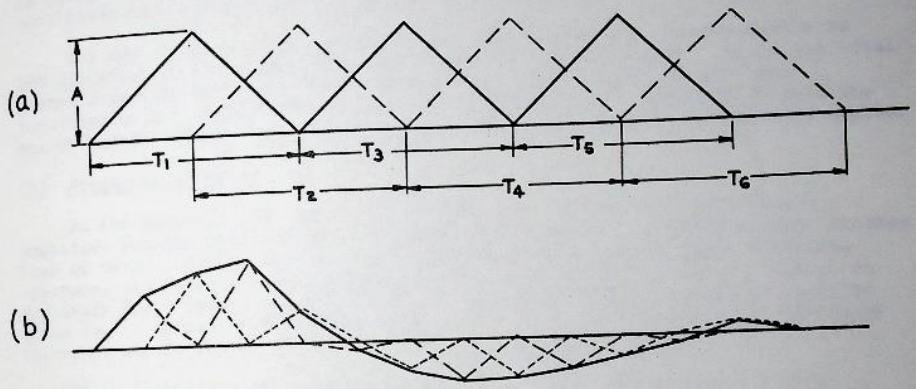

Fig. 6.2.3(ix) Waveforms at output of converter.

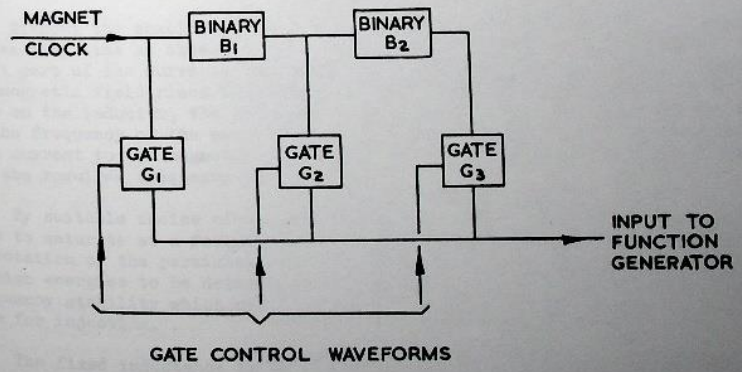

Fig. 6.2.3(x) Block diagram of gate and scaling unit.

The integrator has a jitter equivalent to 30 milligauss, corresponding to 150 c/s in oscillator frequency; the jitter in the voltage to current converter is 8 μA, corresponding to 80 c/s; the amplitude of the f.m. noise in the oscillator is 10 c/s, and the measuring error is 60 c/s.

The sum of these components, assuming they combine in a random manner is 180 c/s which is not in good agreement with the measured value. Since the total jitter figure is well below the assumed limit, this anomaly has not been investigated but could well be due to the difference in environment between the measurements taken on the individual units and those taken on the combined system.

(b) Frequency tracking

As the magnetic field rises after injection, the betatron oscillation amplitude becomes less and small frequency errors can be tolerated without further loss of beam. Taking this into account along with the decrease in effective aperture, the permissible frequency error is shown in Fig. 6.2.4(i). Above an arbitrary field level, say 6 kilo gauss, it can be assumed that further restrictions due to target or extraction requirements will be imposed and the frequency tolerance should follow the curve shown dotted in Fig. 6.2.4(i).

The possible variables are shown in Fig. 6.2.4(ii) where the frequency determining tank circuit of the oscillator is shown in some detail. The oscillator is essentially a Colpitts circuit which is frequency modulated by varying the inductive element. The main variable inductor consists of two ferrite toroids each with a r.f. winding, surrounded by a common polarizing winding. The connections are such that no r.f. voltage is induced in the polarising winding. (This arrangement has been used on other large proton synchrotrons.)

Without the shaping circuit shown in Fig. 6.2.4(ii) the oscillator frequency varies with bias as shown in Fig. 6.2.4(iii)-(a) between 1 and 12 Mc/s. The first part of the curve is very non-linear and is not used (it is traversed while the magnetic field rises from 200 to 300 gauss). By suitable choice of fixed bias on the inductor, the frequency at injection field can be chosen to correspond to the frequency of the particles. Also, by choosing a scale factor relating bias current to the magnetic field, the early part of the curve can be made to fit the required frequency law closely.

By suitable choice of a fixed "shaper" inductance the frequency law can be made to saturate at a frequency corresponding to the near relativistic frequency of rotation of the particles (Fig. 6.2.4(iii)-(b)). This enables the frequency at high energies to be determined by a fixed inductor with a correspondingly high frequency stability which can be adjusted relatively independently of the settings made for injection.

The fixed inductance is further shunted by a small capacitor so that the resonant frequency of the two is slightly above the asymptotic frequency. The combination may therefore be used to adjust the degree of 'squareness' of the knee of the frequency curve as shown in Fig. 6.2.4(iii)-(c). Curve 1 corresponds to the case where the self resonant frequency of the combination is closer to the asymptotic frequency than it is for curve 2. The range of adjustment covers the

theoretical curve so that the components can be set to give an optimum fit. There is a slight disadvantage in that the adjustment of final frequency and degree of squareness are not independent.

The adjustments available on the oscillator can then be summarised as follows:-

(i) an arbitrary choice of the constant of integration to give the correct starting frequency

(ii) choice of the scale factor relating biassing current to magnetic guide field to give optimum tracking over the first phase of acceleration

(iii) adjustment of the final frequency

(iv) adjustment of the squareness of the knee

The optimum adjustment of these controls gives a curve with a tracking error indicated by the points marked in Fig. 6.2.4(i). It can be seen that over the first part of the cycle the points lie inside the curve corresponding to no loss. The maximum deviation from the correct curve is 4% and this is compensated for by the function generator. This applies a correcting signal to the voltage sensitive capacitor, shown in Fig. 6.2.4(ii) as the variable capacitor shunting the tank circuit of the oscillator.

The maximum correction that the function generator (or curve corrector) can apply is 5% and its stability is 0.5% of full scale so the final adjustment should be well inside the curve of Fig. 6.2.4(i).

(c) Final frequency

At the end of acceleration, factors in addition to retention of the beam apply. For example, if the final frequency has a jitter of 0.05% this corresponds to 1 cm in equilibrium radius and would have no effect on beam intensity. However, with a long output pulse, say 500 ms, it would result in a jitter in the timing of the output pulse of the order of 50 ms.

The oscillator circuit is such that the final frequency is determined by "fixed" components which should give high stability. Measurements have confirmed a cycle to cycle jitter in final frequency which corresponds to less than 1 mm of equilibrium orbit radius.

(d) Frequency modulation noise

The phase motion of the particles is a lightly damped oscillatory motion which is excited by frequency and phase modulations of the accelerating voltage. Though the phase oscillation frequency varies over the range 2 to 5 kc/s during the acceleration period, the forcing function is wide band noise which contains components at this frequency at all times. The phase motion is therefore continually excited during the acceleration period.

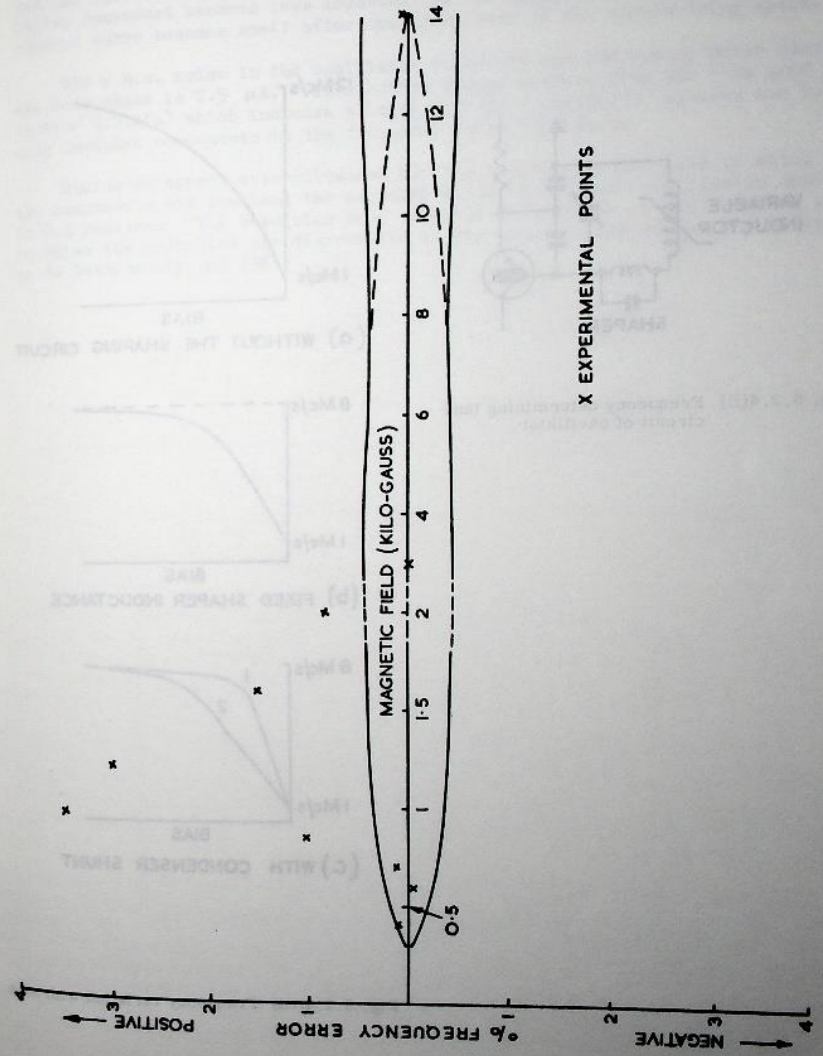

Fig. 6.2.4(i) Permissible frequency error during current rise.

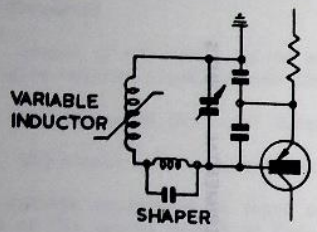

Fig. 6.2.4(ii) Frequency determining tank circuit of oscillator.

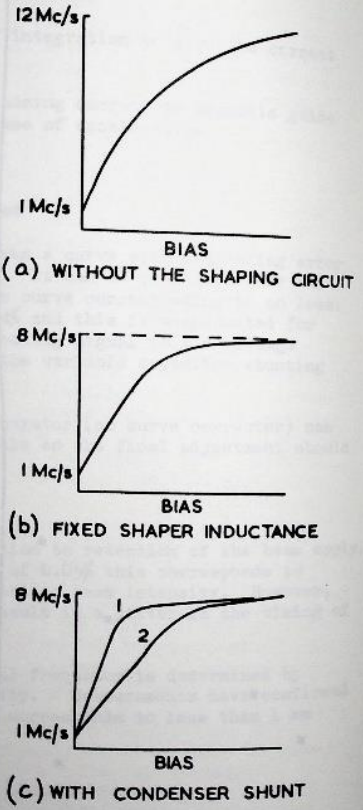

Fig. 6.2.4(iii) Frequency variation with bias.

The noise consists of two components; the inherent noise of the oscillator and the current noise in the amplifying chain providing the bias current. The latter component becomes less important as the slope of the frequency/bias current curve becomes small after the first part of the accelerating cycle.

The r.m.s. noise in the oscillator is 10 c/s and the r.m.s. noise current in the bias chain is 2.5 μA. This latter figure differs from the 8 μA used in section 6.2.4(a) which includes a large "flicker" component, whereas the 2.5 μA only includes components in the frequency range 1-10 kc/s.

Making an approximate allowance for the relative proportions in which these two components are combined the expected build up of phase oscillation amplitude is 0.4 radians. The resulting loss of particles depends on the detailed way in which the particles are distributed in the phase stable region but is expected to be between 10% and 25%.

6.3. High Power R.F. System

6.3.1. Introduction

The high power r.f. equipment comprises the r.f. cavity, the power amplifier, and the bias supply. A block diagram is shown in Fig. 6.3.1(i) and a cut away view of the cavity in Fig. 6.3.1(ii). The single two-gap accelerating cavity is energised from the power amplifier and automatically tuned by the bias supply. The bias supply is controlled by a phase detector sensing the load susceptance. There is also a closed loop amplitude control associated with the power amplifier, acting directly from the gap voltage.

The r.f. frequency programme and also a level control programme are fed to the power amplifier from the primary frequency generator (see section 6.2). The required frequency rises from 1.423 Mc/s to 8.012 Mc/s in 0.75 s; this is repeated every 2 s. The required energy gain per turn averages 6 keV, being proportional to $\dot{B}$. Special voltage programmes may be required at injection and extraction; the system is required to function over a 10:1 range of amplitude at injection. The normal r.f. stable-phase angle is 150°.

The r.f. frequency is the fourth harmonic of the proton orbital frequency. This harmonic number was chosen as the best compromise between the reduction of synchrotron oscillation amplitude and the deterioration of ferrite properties with increasing frequency.

6.3.2. Accelerating Cavity (Figs. 6.3.2(i), 6.3.2(ii)

(a) Basic description

Initially a critical comparison was made between the loaded cavity type structure and the "Bevatron-type" drift-tube structure. It showed the cavity structure was obviously the more efficient (1). This is mainly due to the large beam aperture in Nimrod coupled with the relatively short straight section which would make a low impedance circuit inevitable with the drift-tube arrangement, leading to a necessity for a high peak voltage and hence a high power requirement.

A third alternative, consisting of a cavity incorporating a variable capacitor, was also considered and rejected because of awkward mechanical problems which would introduce jitter and noise. The power requirement would again be high because the ferrite would be less heavily biased (and therefore more lossy) at high frequencies and the capacitance at low frequencies would be higher, leading to a lower impedance.

The loaded cavity consists of two highly re-entrant E_{010} resonators side by side. They are loaded symmetrically by a total of four ferrite cores to provide a large variable inductance. The capacitance is not varied. The two accelerating gaps are paralleled and connected to the output of the push-pull amplifier. The ferrite is biased by a d.c. winding which links the two cavities in opposite senses, to buck out r.f. voltages. The d.c. winding is distributed round the cores and being inside the cavity, it also acts as the main r.f. winding (its turns are paralleled by capacitors for this purpose) and the cavity walls can be

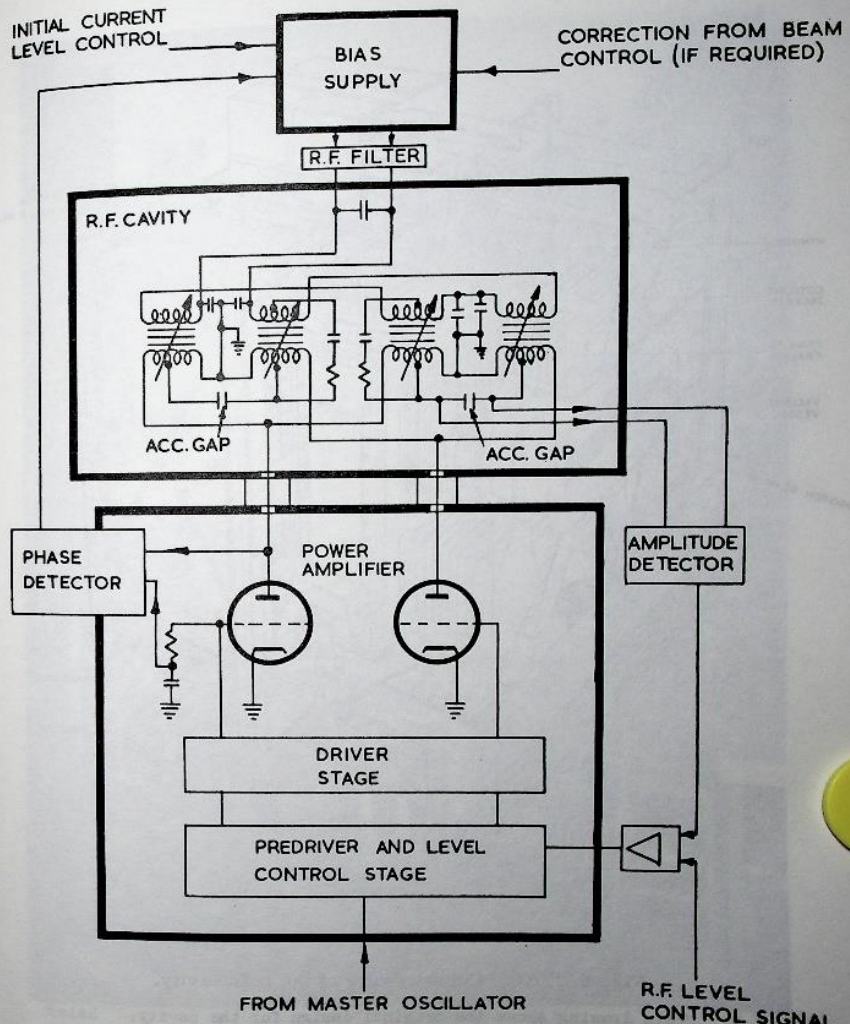

Fig. 6.3.1(i) Block diagram of high power r.f. system.

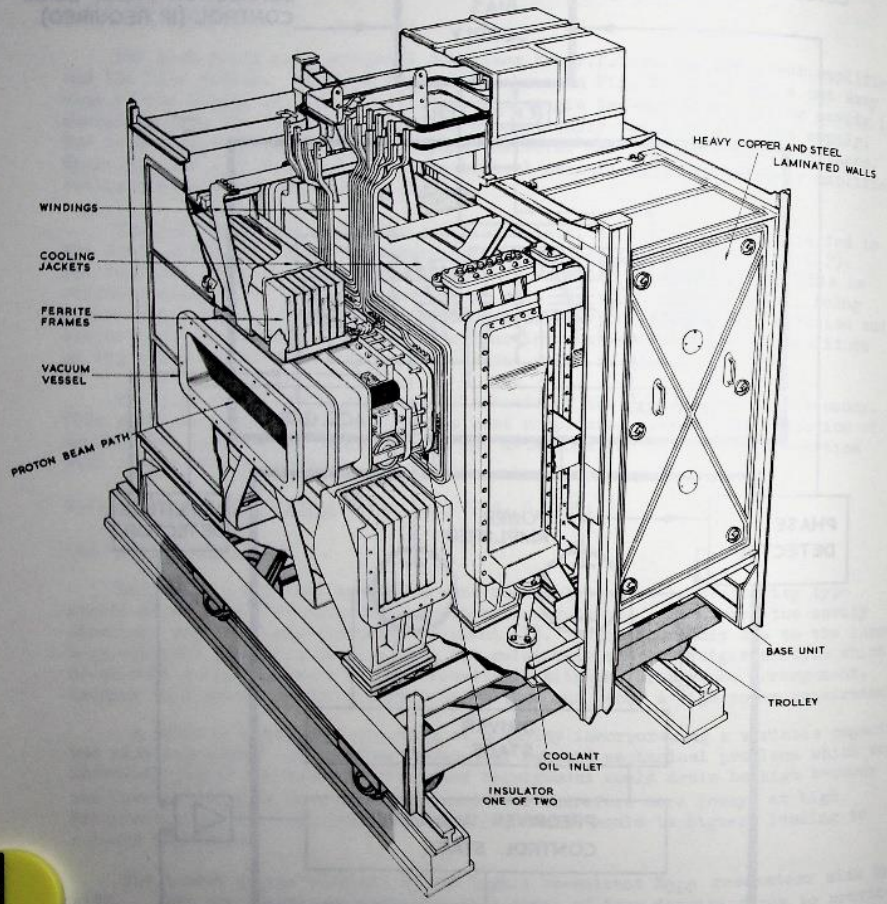

Fig. 6.3.1(ii) Cutaway view of the r.f. cavity.

N.B. This drawing shows the original design for the cavity. Later modifications included new side covers, removal of tuning capacitors and addition of separate r.f. windings (see para. 6.3.2).

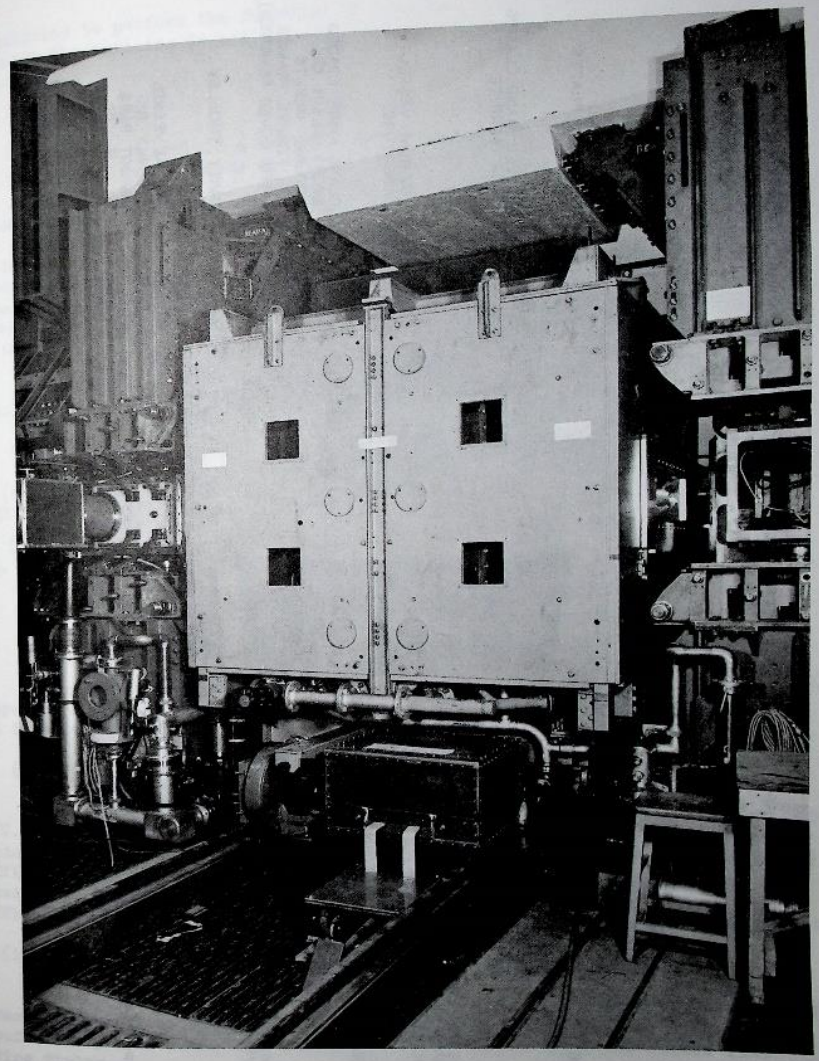

Fig. 6.3.2(i) View of the accelerating cavity in position in straight section 8.

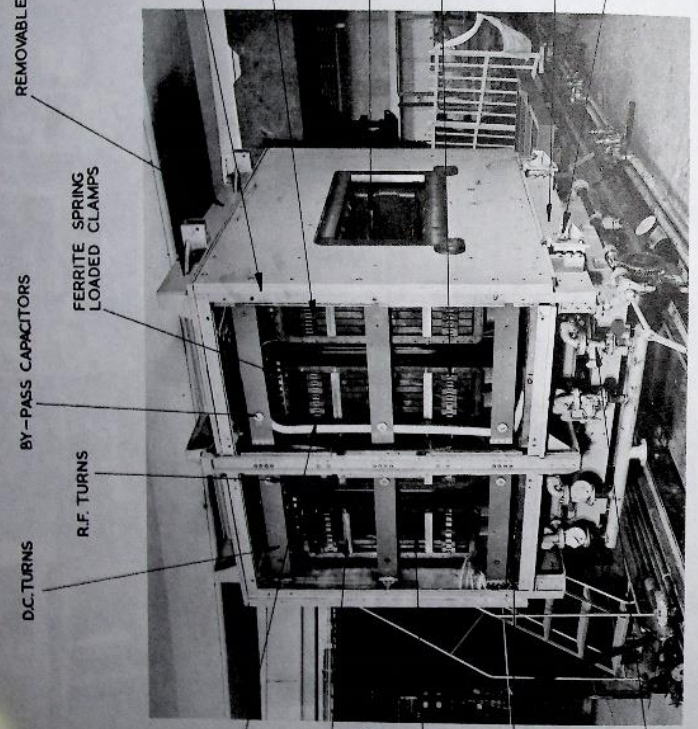

Fig. 6.3.2(ii) View of the accelerating cavity.

considered to perform the function of a screen. The central dividing wall between the cavities is not present, as it performs no useful electrical function.

(b) Vacuum vessel

The vacuum vessel is a rectangular cross section stainless steel tube with two insulating gaps, across which the accelerating voltage is developed. When the cavity is moved out of its position in the magnet ring for servicing, the vacuum vessel can be rolled on wheels out of the cavity (in the beam direction) for inspection of the insulators and seals. The wheels run in locating grooves on the epoxy resin boxes enclosing the ferrite. Large spring fingers make electrical connections to the end walls of the cavity. Various materials were considered for the insulators including glass, fibre-glass and epoxy resin, alumina and other ceramics, polythene and P.T.F.E. The principal requirements of the material are that it shall have:-

(i) a combination of low dielectric loss and high thermal conductivity, i:e. $(\varepsilon \tan\delta)/K$ must be as small as possible;

(ii) low vapour pressure and gaseous permeability;

(iii) reasonable mechanical strength, freedom from plastic flow and a high radiation resistance;

(iv) suitable properties to allow manufacture to the shape shown in Fig. 6.3.2(iii).

The results of the investigations were as follows:-

(i) Glass fibre and epoxy resin

The choice of an epoxy resin was abandoned since experiment showed that the temperature rise of at least 90°C. would lead to a very high vapour pressure and that a fairly extensive air blowing system would be required.

(ii) P.T.F.E.

This material would have a temperature rise during operation of approximately 22°C. which, together with a surface temperature of 20°C., might just be satisfactory from a vacuum point of view, although the vacuum seal could have proved difficult due to plastic flow of the P.T.F.E. A number of manufacturers were asked to produce an insulator of this material but they declined, due to difficulties in making a suitable mould. P.T.F.E. also has poor radiation resistance.

(iii) Alumina ceramic

Several types of ceramics satisfied the principle requirements, although the gaseous permeability could have proved troublesome in some cases. Again manufacture proved difficult, mainly due to the break up of the formed item during firing.

(iv) Glass

A special telescopic glass slab, having good vacuum and r.f. qualities and high radiation resistance, was manufactured. Insulators were cut from this slab and proved satisfactory when tested under the operating conditions expected in the r.f. cavity. The cost of this type is, however, rather high.

(v) Polythene

Polythene insulators have been adopted and are in use but glass ones are available as an alternative. The polythene insulators have proved satisfactory under operating conditions although the effect of radiation is not yet known.

Insulator tests

All insulators were subjected to vacuum and high voltage tests on a test rig in which the insulator was secured between two stainless steel vessels by 32 tie bars. One of the vessels was fitted with a diffusion pump provided with a refrigerated baffle. Both the cavity vacuum vessel and the insulator test rig vacuum vessels have special metal stops fitted, equally spaced, around the inner faces to prevent excessive strain on the insulators when under vacuum. With both polythene and glass insulators a vacuum of 5×10^{-7} torr was achieved after about 48 h pumping.

High voltage tests were carried out using a portable r.f. transmitter with an output power sufficient to produce approximately 8 kV across the insulator. During these tests the vacuum vessels were carefully insulated and screened by a copper box.

The test rig was eventually modified so that it can be attached to the cavity vacuum vessel when the cavity is withdrawn from the magnet ring to its test position in the centre of the magnet hall. Under these conditions the normal cavity power amplifier is available to provide a source of r.f. voltage, since it remains attached to the cavity.

Tie Bars

The original specification for the 32 tie bars securing each insulator between the flanges of the cavity vacuum vessel called for a material having a low dielectric constant and a low power factor to avoid overheating when placed in a r.f. field. Ceramic and epoxy resin glass fibre types were tested, the latter proving the better both for mechanical strength and r.f. properties. The breaking strain of each tie bar is 5 ton.

Each end of a tie bar is provided with a split collar and a special nut which is tightened only by means of a torsion spanner while the collar is held in place by a tool provided. Abrasion and scoring of the tie bar ends by the split collars has been overcome by binding the ends with a single turn of 0.002 in. aluminium alloy strip before assembly.

The bars have a relatively large surface area to cross section ratio and do not overheat but a little air is blown over them as a safety precaution.

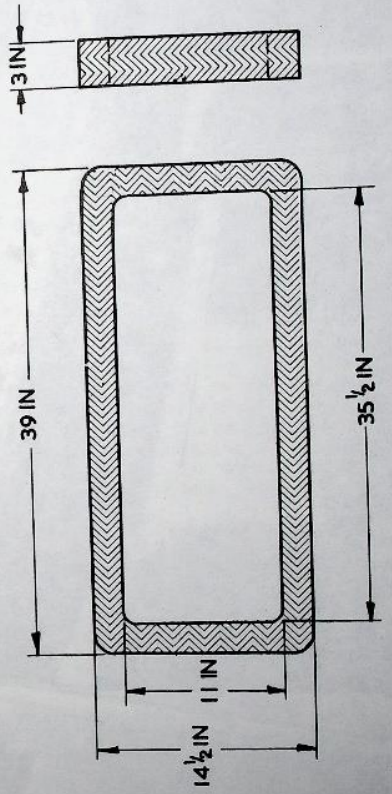

Fig. 6.3.2(iii) Shape of vacuum vessel insulators.

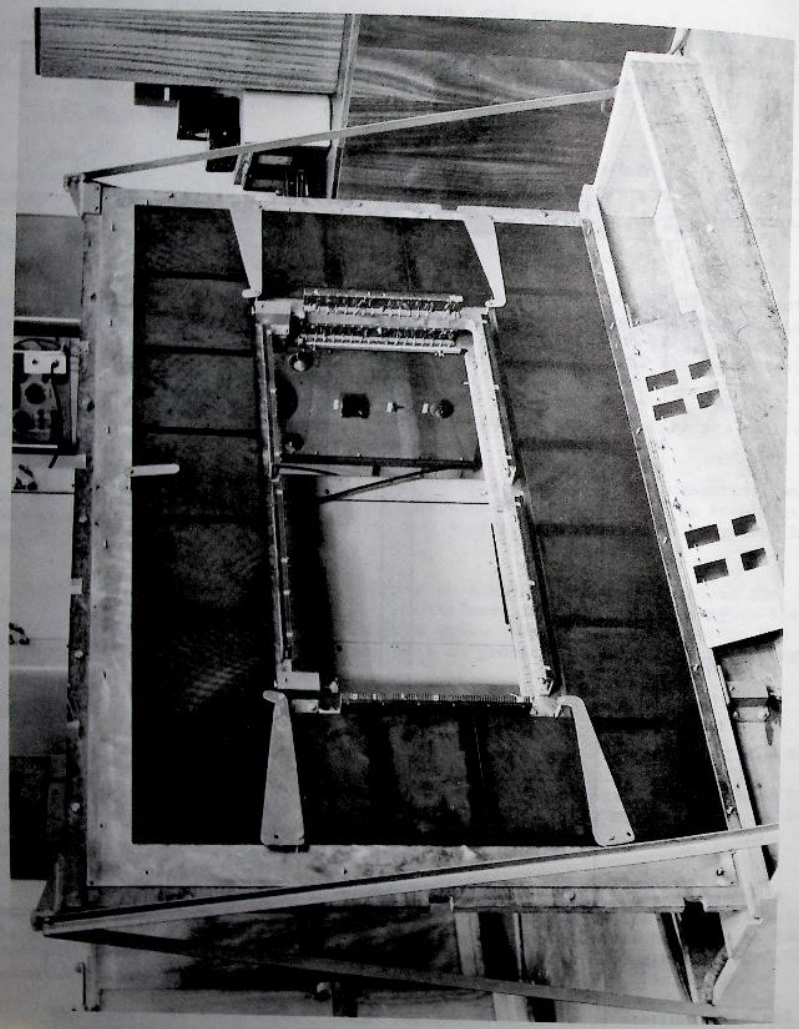

Fig. 6.3.2(iv) View of a ferrite core 'window frame'.

(c) Ferrite

A careful investigation was made of all available materials. A full account of this investigation has been reported elsewhere (2). The requirement was for the best compromise for the product μQ over the frequency range and the ampere turns required to pull the resonant frequency from 1.4 to 8.0 Mc/s. (μ = permeability of ferrite; Q = loaded Q of complete cavity with ferrite filling). It was also necessary for the manufacturer to be capable of manufacturing large blocks to the required mechanical and electrical tolerances. The material finally chosen was a special Philips material similar to Mullard B_1, but with a slightly lower permeability and correspondingly higher Q. At 1.4 Mc/s unbiased: μ = 600 and Q = 10 at 60 gauss peak flux density. When biased to 8.0 Mc/s: Q = 40 and the bias field is 12 AT/cm. The ferrite is made in "window frames" 4 cm thick (Fig. 6.3.2(iv)). The long limbs are each made of seven blocks (25 cm by 23 cm) and the short limbs of three narrower blocks. The four limbs of a window frame are loaded individually into the cavity and are held together by gravity and by spring loaded clamps on the top surface.

A problem arose over the joining together of the blocks to form limbs. Originally all the limbs were made by glueing the blocks together with cold-setting Araldite. However, during assembly into the cavity some of the long limbs broke in the centre, and it was found after an extensive investigation by the manufacturers that the strength of the cold-setting Araldite bond decreased with time, reaching zero after a period of 4 or 5 weeks, due to water vapour from the air reaching the bond through the porous ferrite. A technique was developed for glueing the limbs using a hot setting Araldite, which also loses some strength during the first few weeks after glueing but levels off at a value which is still very high. However, in the meantime a method had been found to hold the long limbs together using stainless steel clamps. These clamps were sufficiently small to fit in the cavity without affecting the oil flow around the ferrite, and they included an insulating portion to avoid the possibility of induced currents in the clamps. The short limbs rely on gravity to assist the strength of the original Araldite bond.

There are 28 frames in the cavity (7 in each core), with a total weight of nearly 6 ton. The amount of r.f. power absorbed by the ferrite varies with frequency but has a peak value of about 42 kW at 4.5 Mc/s. The four ferrite cores are enclosed in individual fibre-glass loaded epoxy resin jackets filled with transformer oil, which is cooled by circulation through a heat exchanger, the inlet temperature being maintained at 58°F (14.5°C).

(d) Bias Winding

The ferrite requires a total bias field of approximately 7,000 AT. If this were provided by a single winding carrying 7,000 A the peak voltage required to obtain the desired rate of rise of current would be approximately 5 V. The cavity was designed and built in such a manner that the actual cavity walls could be used as a single turn winding of this type, but it was decided that the most convenient impedance at which to work would be provided by a 10-turn winding requiring a peak current not exceeding 800 A and a peak voltage of 50 V and this was the arrangement finally used. The path followed by any one turn of the winding is shown in Fig. 6.3.2(v). The input is underneath the centre of the cavity and the 10 turns are distributed circumferentially around the ferrite. The input is bypassed with a 0.01 μF capacitor, and is connected through the r.f. filter

to prevent even small r.f. currents getting to the sensitive operational amplifiers in the bias supply. There is a considerable problem in avoiding subsidiary resonances in the bias winding system. These, in general, are due to the air-cored stray inductances and capacitances between sections of winding and the adjacent cavity wall. The bias winding is the main conductor for r.f. currents, and to ensure a uniform current distribution the windings are paralleled for r.f. by 0.01 μF capacitors.

In addition, each winding is decoupled to the cavity wall. Originally each was decoupled in at least two places and also bypassed to the actual flange of the accelerating gap. This combination lead to the existence of a host of absorption resonances in the 1 to 8 Mc/s band, giving a low input impedance at some frequencies and high voltages at certain decoupling capacitors. It was found that owing to the complex arrangement of the bias winding turns within the cavity, it was impossible to eliminate all resonances within the 1 to 8 Mc/s band from the cavity.

After removing all except one decoupling capacitor on each turn, and bypassing only one of the turns to the gap flange, most of the resonances disappeared. However, to eliminate one severe "double-humping" condition associated with the central part of the vacuum vessel, it was necessary to bypass the winding to the gap flange on the inner side only of each gap. This latter bypass capacitor circuit was found to carry a very large current at one frequency and to prevent the capacitor being destroyed in the event of the cavity being energised continuously at this frequency, a 2Ω , 200 W damping resistor was inserted.

Lesser resonances were found to overheat some of the other decoupling capacitors at certain frequencies and eventually a simple filter arrangement was used between each turn and the wall, consisting of a 0.01 μF capacitor in series with a parallel combination of a 0.01 μF capacitor and a 6Ω , 20 W resistor.

(e) R.F. winding

The accelerating gaps in the cavity are connected in parallel by the bias winding and the original intention was to connect the power amplifier directly to the centre point of this parallel connection. This, however, presented a rather low impedance to the power amplifier and it was decided to increase the input impedance of the cavity by making the cavity a two-turn to one-turn, step-down auto-transformer. To accomplish this, each input lead from the amplifier goes once round the appropriate ferrite core before being attached to the flange at the accelerating gap. The configuration of the windings is shown in Fig. 6.3.2.(v) while a theoretical equivalent circuit for the cavity and the bias and r.f. windings is given in Fig. 6.3.2(vi).

The arrangement introduces two new factors; the leakage inductance of the transformer and the stray turn-to-turn capacitance. The effect of the stray capacitance is to lower the resonant frequency of the cavity and all the lumped tuning capacitance which was originally incorporated had to be removed. This was also necessary because the output capacity of the power amplifier is seen by the cavity through the 4:1 impedance transformation. The effect of the leakage inductance is to reduce the voltage at the gaps and also to cause a series resonance to appear when the leakage inductance resonates with the gap capacitance. This resonance tends to occur between 10 and 20 Mc/s and it was decided to push it above 16 Mc/s, i.e. above the second harmonic of the maximum operating frequency. A low inductance winding is required to do this and in the final

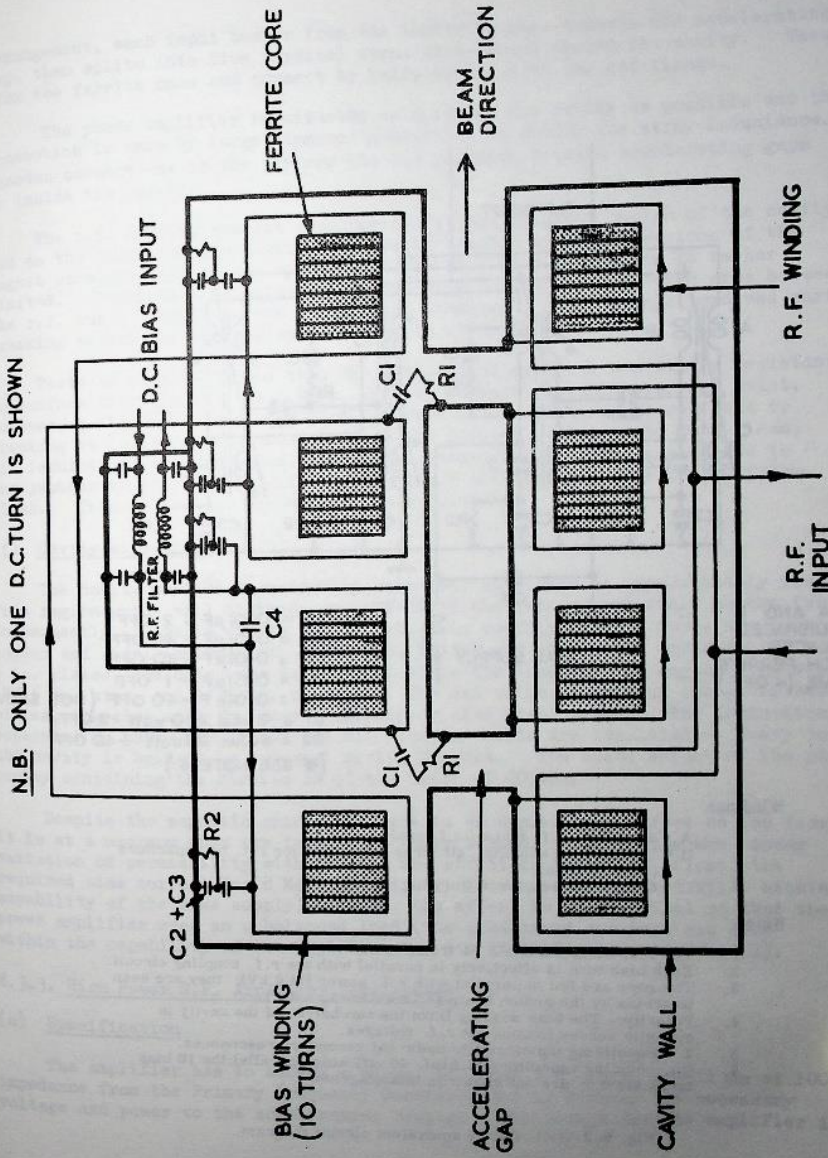

Fig. 6.3.2(v) The winding configuration of the accelerating cavity.

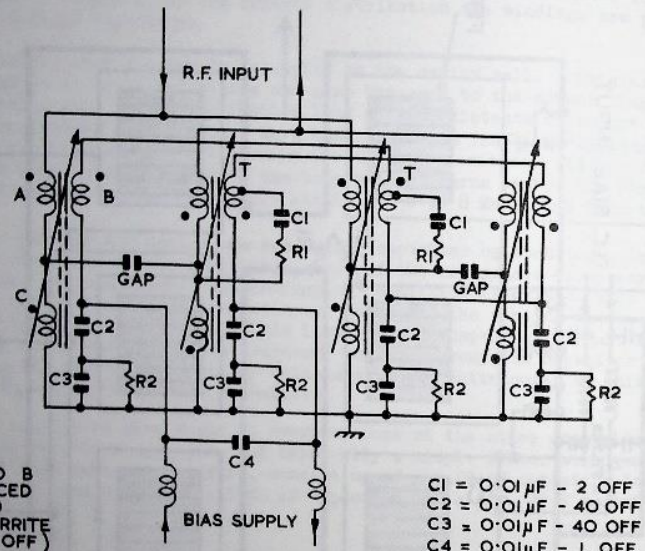

WINDINGS A AND B WOUND EQUISPACED AND INTERLACED ROUND EACH FERRITE CORE FRAME (4 OFF)

C1 = 0·01 μF - 2 OFF
C2 = 0·01 μF - 40 OFF
C3 = 0·01 μF - 40 OFF
C4 = 0·01 μF - 1 OFF
✱ C5 = 0·01 μF - 40 OFF (NOT SHOWN)
R1 = 2 ohm 200 watt - 2 OFF
R2 = 6 ohm 20 watt - 40 OFF
(✱ SEE NOTE 6)

Windings

A = 5 parallel r.f. turns (≡ 1 turn)
B = 10 turn bias winding; all turns paralleled for r.f. by capacitors (≡ 1 r.f. turn).
C = Cavity walls (≡ 1 r.f. turn)

Notes

1. The r.f. turns form a 2 : 1 transformer
2. Each bias turn is effectively in parallel with the r.f. coupling circuit.
3. The gaps are fed in parallel with r.f. power (at 6 kV); they are seen in series by the proton beam (≈ 12 kV for $\phi_s = 30^o$).
4. Polarity:- The bias winding links the two halves of the cavity in opposite senses to buck out r.f. voltages.
5. T = Equalising tap circuit to damp out secondary resonances.
6. C5, coupling capacitors (0.01μf, 40 off) which parallel the 10 bias turns for r.f. are not shown in this diagram.

Fig. 6.3.2(vi) Cavity equivalent circuit diagram.

arrangement, each input busbar from the amplifier goes towards the accelerating gap, then splits into five parallel turns distributed around the cavity. These link the ferrite once and connect by knife switches to the gap flange.

The power amplifier is situated as close to the cavity as possible and the connection is made by large diameter conductors to reduce the stray inductance. To shorten connections to the minimum the tee junction between accelerating gaps is inside the cavity.

The r.f. winding was not incorporated in the original design of the cavity and as the length of the cavity is severely limited by the dimensions of the magnet straight section the space available for the r.f. winding is rather limited. Originally, considerable difficulty was experienced with arcs between the r.f. turns themselves and to the bias winding. These always involved surface tracking across the fibre-glass oil jackets around the ferrite.

Tests on samples showed that the fibre-glass material was highly resistant to surface tracking at 1 to 8 Mc/s, with or without red anti-tracking paint. However, quite small traces of dirt (or more particularly moisture) lead to tracking at quite low voltages. Since the jackets could not be kept clean, air insulation had to be used. Ceramic stand-off insulators were glued to the jackets to support the r.f. turns, with a clearance of $\frac{3}{8}$ in to the fibre-glass. This solved the arcing problem completely.

(f) Cavity screening

The cavity must be magnetically screened, to ensure an approximately field free region which will minimise any effect of the main magnet field on the ferrite. Consequently all walls of the cavity, which is roughly a 7 ft. cube, are made of copper and steel laminations. The top, bottom and side walls are made up from two $\frac{1}{2}$ in. plates, the outer one being steel while the inner one is copper clad steel (7/16 in. steel and 1/16 in. copper). The end walls consist of two $\frac{1}{2}$ in. steel plates, together with an inner $\frac{1}{2}$ in. copper clad steel plate. The laminations are separated by paper insulation and all clamping bolts are insulated. Every joint in the cavity is bridged by internal spring fingers. The total weight of the shielded cavity containing the ferrite is of the order of 20 ton.

Despite the magnetic shielding there is an appreciable effect on the ferrite. It is at a maximum when the ferrite is fully biased, owing to the non linear variation of permeability with flux. The effect is two-fold: first, the required bias current for 8 Mc/s is slightly increased (to values still within the capability of the bias supply), second, the effect is asymmetrical so that the power amplifier sees an unbalanced load (the unbalanced currents are also within the capability of the amplifier and its stability is not affected).

6.3.3. High Power R.F. Amplifier Development

(a) Specification

The amplifier has to accept a signal of about 2 V r.m.s. amplitude at 100 Ω impedance from the Primary Frequency Generator and to deliver the necessary voltage and power to the accelerating cavity. The design for the amplifier is

based on the specification in (3). Important features are displayed in the following figures:-

Fig. 6.3.3(i) shows the peak voltage required plotted against frequency; it is about 6 kV over the band. Fig. 6.3.3(ii) shows the impedance presented to the amplifier plotted against frequency. Each valve of the output stage has an anode load which falls to 250 Ω . Fig. 6.3.3(iii) shows the power loss which is almost entirely absorbed in the ferrite cores; the skin loss and beam loading effects are negligible by comparison. The graphs in the last two figures were based on estimates from a sample ferrite testing programme. Fig. 6.3.3(iv) shows the assumed equivalent circuit for the cavities. It was decided at an early stage that to assess the behaviour of the cavities, the amplifier must be capable of operating with a c.w. output. In considering the valve line-up therefore, no account is taken of the 3:1 duty factor in the actual machine cycle.

From Fig. 6.3.3(i) and (ii) allowing a safety margin, the most stringent peak conditions for each output valve of the amplifier are:-

Required anode swing	=	3.5 kV
Load impedance	=	250 Ω
Fundamental component of anode current	=	14 A (peak)

Considering only triodes: for a reasonable angle of anode current flow, the peak space current to meet the above condition could be 35 A which demands a high peak usable cathode current. A low anode efficiency and high peak grid current would follow and would require a high input driving voltage. There is the further problem of the input capacitance of these large valves, since a wideband untuned stage would be needed to drive the output stage of the amplifier. If a conventional push-pull amplifier is correctly cross-neutralised the input capacitance = $2(C_{ga} + C_{gf})$ + strays (say 200 pF total). There is, therefore, a large reactive current demand from the driver at 8 Mc/s.

Further examination of the likely load impedance leads to the decision to incorporate a 4:1 impedance transformation ratio into the cavities by carrying the input leads once round the ferrite cores before connecting them to the accelerating gaps. Each valve then runs under the following conditions:-

Required anode swing	=	7 kV
Load impedance	=	1000 Ω
Line current	=	7 A (peak)

At this stage an analysis was carried out as described in (4). The analysis covered a wide range of possible valves and a large number of possible operating conditions. The final choice was the English Electric Co. Type BW 161 with the following specification:- V_a max = 12 kV; Anode dissipation = 30 kW; Peak usable cathode current = 45 A; G_m = 23 mA/V; μ = 45; C_{ga} = 36 pF; C_{gf}=57 pF. The basic circuit arrangement used is shown in Fig. 6.3.3(v). To prove the power output capability of this circuit it was tested using a dummy load as shown in Fig. 6.3.3(vi). This load had impedance v. frequency and Q factor v. frequency characteristics similar to those of the cavity.

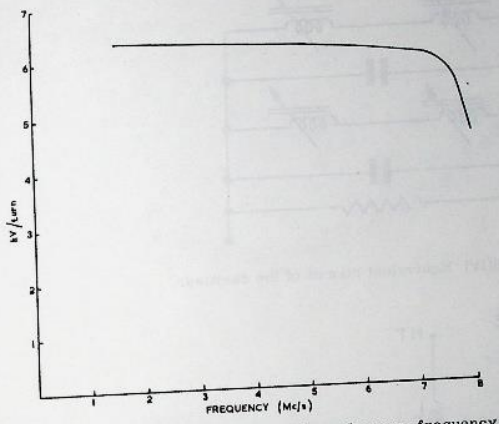

Fig. 6.3.3(i) Required accelerating voltage v. frequency.

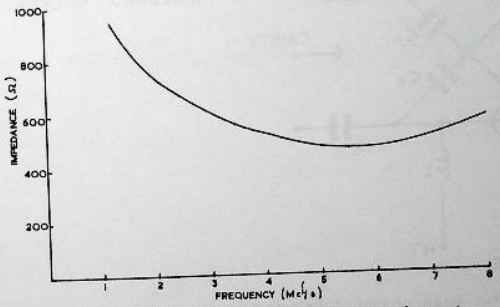

Fig. 6.3.3(ii) Cavity load impedance v. frequency.

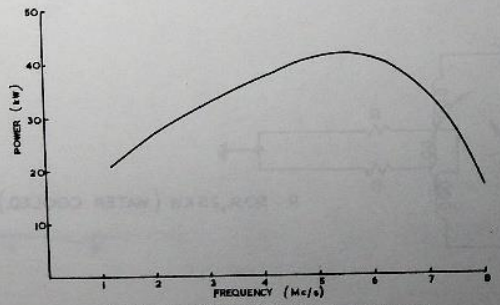

Fig. 6.3.3(iii) Power loss v. frequency.

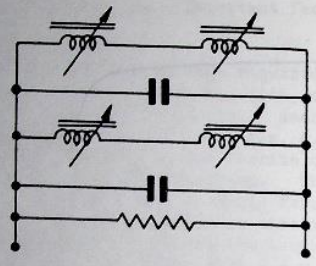

Fig. 6.3.3(iv) Equivalent circuit of the cavities.

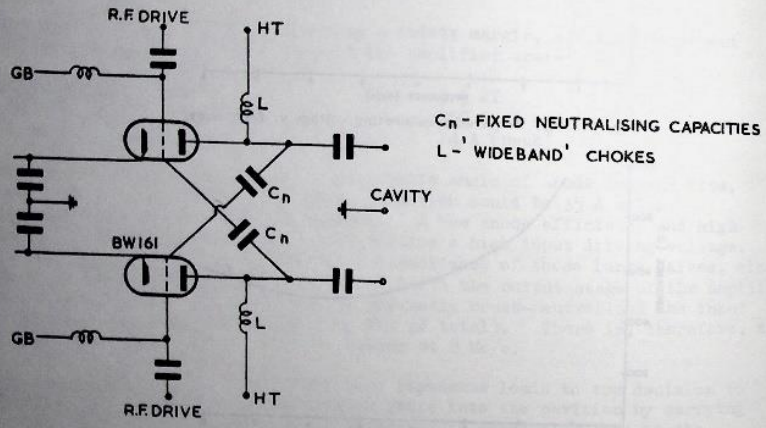

Fig. 6.3.3(v) Basic circuit of the output stage.

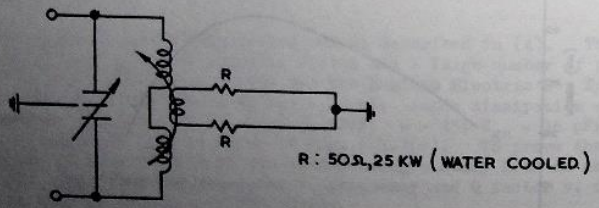

Fig. 6.3.3(vi) Dummy load for tests on amplifier output stage.

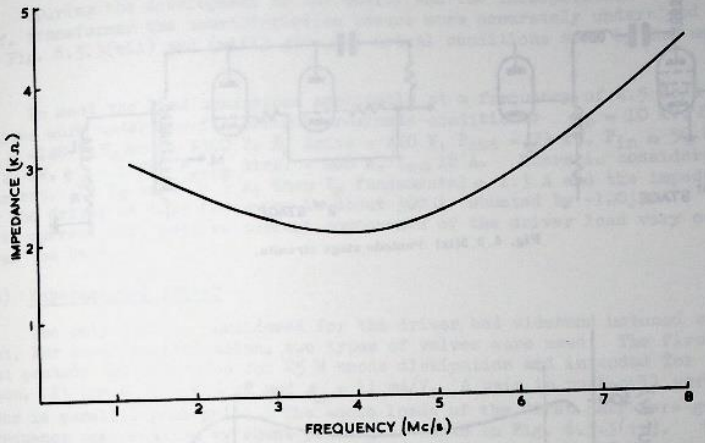

Fig. 6.3.3(vii) Actual load impedance v. frequency.

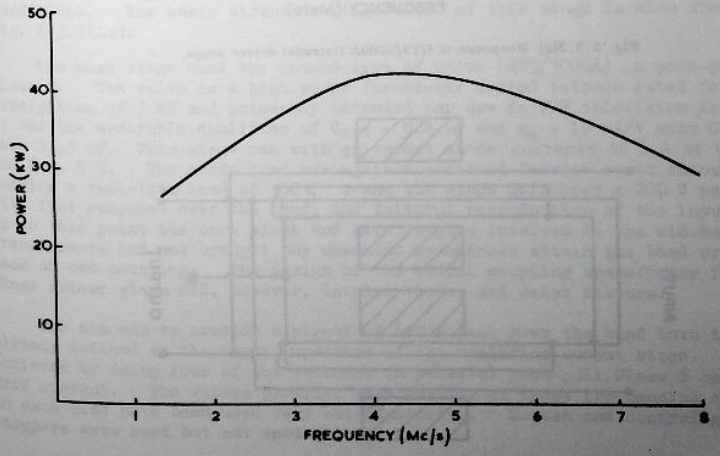

Fig. 6.3.3(viii) Actual power loss v. frequency.

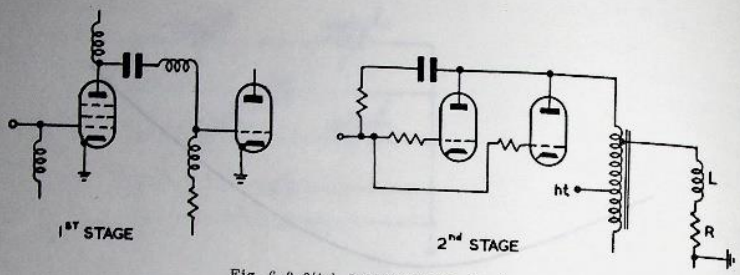

Fig. 6.3.3(ix) Pentode stage circuits.

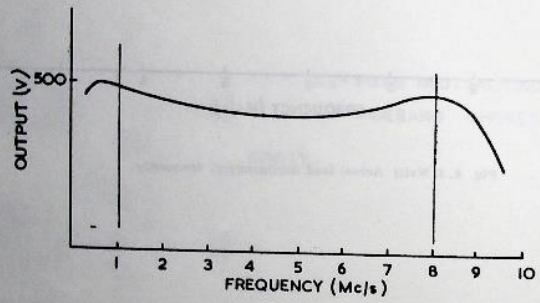

Fig. 6.3.3(x) Response of QY5/3000A (tetrode) driver stage.

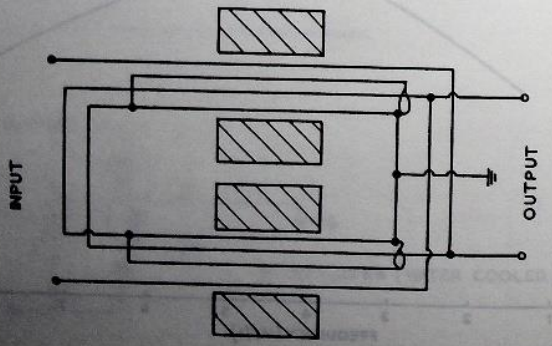

Fig. 6.3.3(xiv) Winding arrangement on the driver output transformer.

During the development of the cavity and the incorporation of the integral r.f. transformer the characteristics became more accurately understood and the graphs in Fig. 6.3.3(vii) and (viii) give the actual conditions seen by the amplifier.

To meet the load conditions applicable at a frequency of 4.5 Mc/s, the output valves work under the following approximate conditions:- V_b = 10 kV, E_a min = 3 kV, V_c = -140 V, E_g max. = +300 V, E_g drive = 440 V, P_{out} = 23 kW, $P_{in} \triangleq$ 50 kW, P_a diss. = 27 kW, $\theta_p = 180°$, P_{grid} diss. = 200 W, $I_m \triangleq$ 18 A. There is considerable grid current. If I_g total = 3 A, then I_g fundamental $\triangleq$ 1.3 A and the impedance seen by the driver at this frequency is about 300 Ω shunted by -120j Ω . Both the grid current and reactive current components of the driver load vary considerably over the band.

(b) Experimental driver

The only designs considered for the driver had wideband untuned stages throughout. For power amplification, two types of valves were used: The first was an output pentode (EL 34) rated for 25 W anode dissipation and intended for audio reproduction. It has C_{out} = 8.4 pF and g_m = 11 mA/V. A pair in push-pull were used to drive four in parallel push-pull. The anode loads of the first pair were given high frequency compensation by shunt peaking as shown in Fig. 6.3.3(ix). The anode load of the second stage was an autotransformer feeding an inductance peaked resistive load which was designed to swamp the input impedance of the succeeding stage. The resistance value was 300 Ω . The output transformer used two tape wound coil stacks side-by-side on a small toroidal ferrite core and the stage delivered a 70 V peak signal to the succeeding stage with a flat response over the band. Feedback was used to improve linearity and to maintain a good sinusoidal waveform in the output; the second of the two stages ran under Class A conditions. The basic circuit configuration of this stage is also shown in Fig. 6.3.3(ix).

The next stage used the second type of valve (QY5/3000A) in push-pull and Class A. The valve is a high power forced-air cooled tetrode rated for anode dissipation of 3 kW and primarily intended for use in VHF television transmitters. It had the desirable qualities of C_{out} = 8.4 pF and g_m = 19 mA/V with C_{in} no more than 23.5 pF. This stage ran with quiescent anode currents of 1 A at V_b = 2 kV and E_c = 0 V. The anode load was again a wideband ferrite cored autotransformer feeding a resistive load of 300 Ω , and the stage delivered a 200 V peak signal with flat response over the band, and faithful reproduction of the input waveform. Up to this point the core sizes and wire lengths involved in the wideband transformers had not brought any unwanted resonances within the band or caused lack of end coupling. The design of the output coupling transformer for the final driver stage did, however, involve these, and other factors.

The aim was to provide a signal of 600 V peak over the band into the load already defined as the input impedance of the amplifier output stage. This was achieved by using four of the tetrodes in parallel push-pull, Class B condition, with grid current. The valves parallel very readily at these frequencies and three on each side have been used very satisfactorily. Screen and control grid stoppers were used but not anode stoppers.

To keep the flux swing in the output transformer core to a reasonable level the core was necessarily large and the leakage inductance and winding capacitances were high. The toroidal core size was 150 mm OD, 50 mm ID, 40 mm thick and carried a total of 32 turns of wire. The leakage inductance of this transformer was arranged to resonate with the input capacitance of the final amplifier BW 161 tubes and for a level input over the band the driver output stage produced a response curve as shown in Fig. 6.3.3(x). It shows a characteristic peak below the bottom frequency of the band due to shunt winding resonance, then a slight droop and a flattened peak just above 8 Mc/s. The flattening was achieved by resistors placing 350 Ω across the transformer primaries and has the effect of maintaining the screen currents of the tetrodes at an acceptable level throughout the band.

Complete circuit diagrams for the prototype transmitter are given in Figs. 6.3.3(xi), 6.3.3(xii) and 6.3.3(xiii). This driver and output stage was used successfully through all the early testing of the cavity, the automatic gap voltage control and the automatic cavity tuning system.

(c) Wide band transformer development

Further work was carried out on the driver output transformer and a large number of winding and core configurations were tried. The following design considerations were incorporated in the transformer. It would couple the anodes of six of the tetrodes connected in parallel push-pull to the grids of the BW 161 valves and give a flat response over the range 1.4 Mc/s to 8 Mc/s. The use of transformer coupling enables a leakage inductance to be selected which will separate the output and input capacitances of the stages to be coupled to form a π network at the upper frequencies. In this way it is possible to achieve a flat response characteristic over the band and to introduce a transformation ratio to accommodate the difference between the two capacitances. At an upper frequency limit of 10 Mc/s the reactance of the 200 pF looking into each BW 161 is 80 Ω. The load resistors from each grid to ground were therefore fixed at 75 Ω.

The total anode capacitance of each side to ground is 100 pF, the reactance at 10 Mc/s being 160 Ω. Together with strays, this gives an anode-anode impedance of 300 Ω. The impedance ratio required for the transformer is therefore 300:150 Ω; a turns ratio $\sqrt{2}$:1 The nearest possible figure with the low number of turns required is 1.5:1.

The transformer must handle a peak drive voltage to each BW 161 of 500 V. The total r.m.s. drive power is therefore 3300 W. The transformer losses must be kept low because of heating and for efficiency. It was manufactured on a core consisting of eight ferrite toroids each having OD = 3 in, ID = 1 in and axial length 1.57 in. These were arranged in binocular form with concentric and strip windings to give limited impedance matching through the windings.

The transformer design met the specification and could be overloaded to deliver 1000 V from each output terminal to ground at 6.3 Mc/s. The basic winding arrangement is shown in Fig. 6.3.3(xiv).

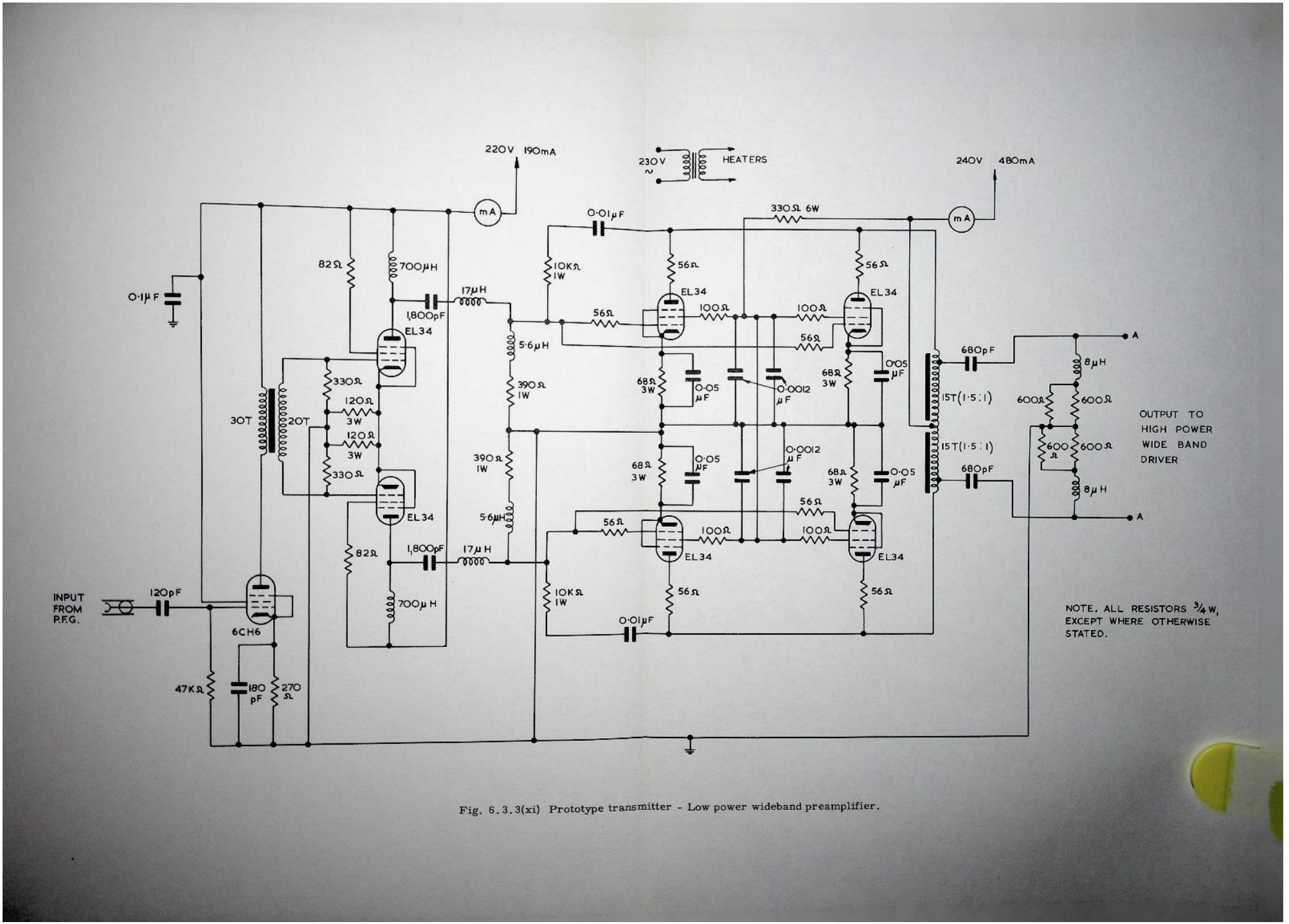

Fig. 6.3.3(xi) Prototype transmitter - Low power wideband preamplifier.

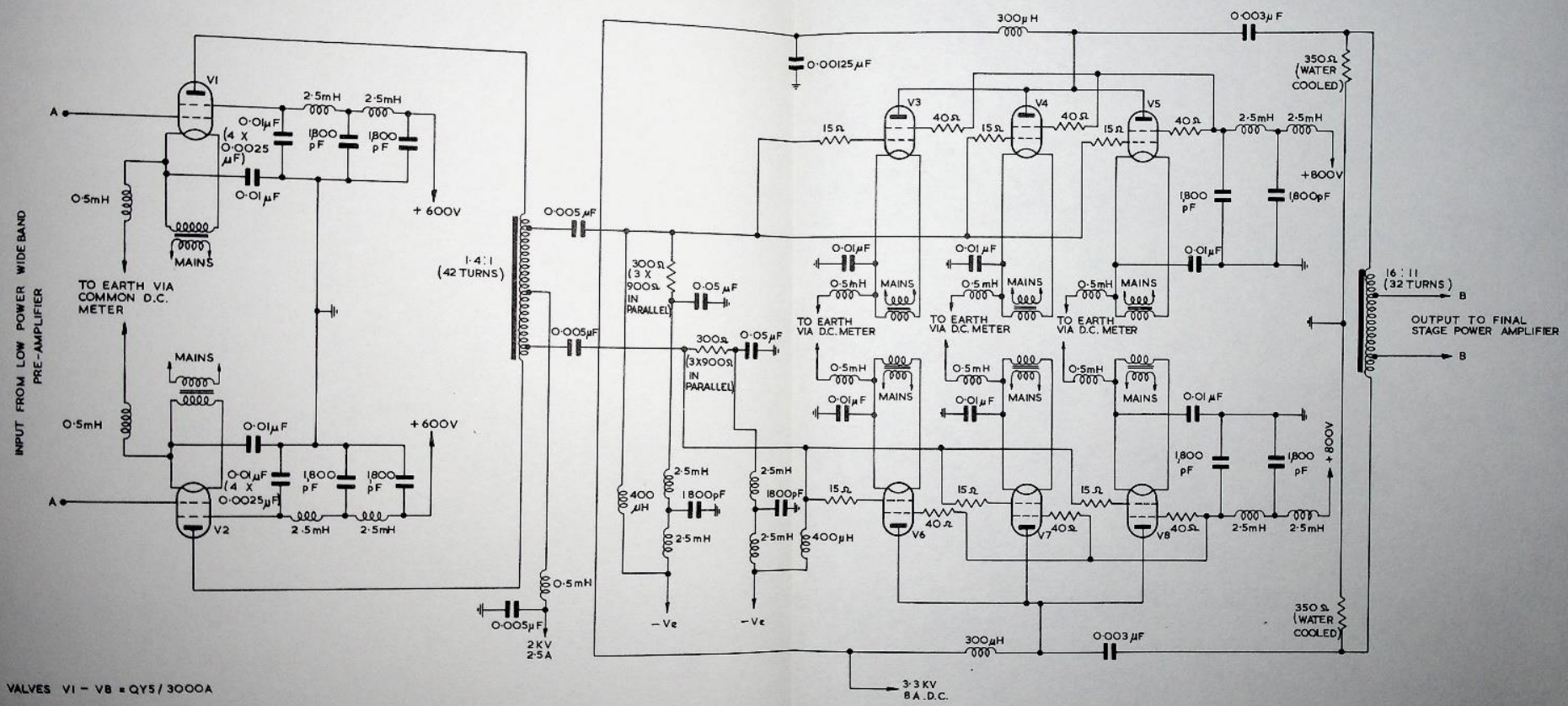

Fig. 6.3.3(xii) Prototype transmitter - High power wideband driver.

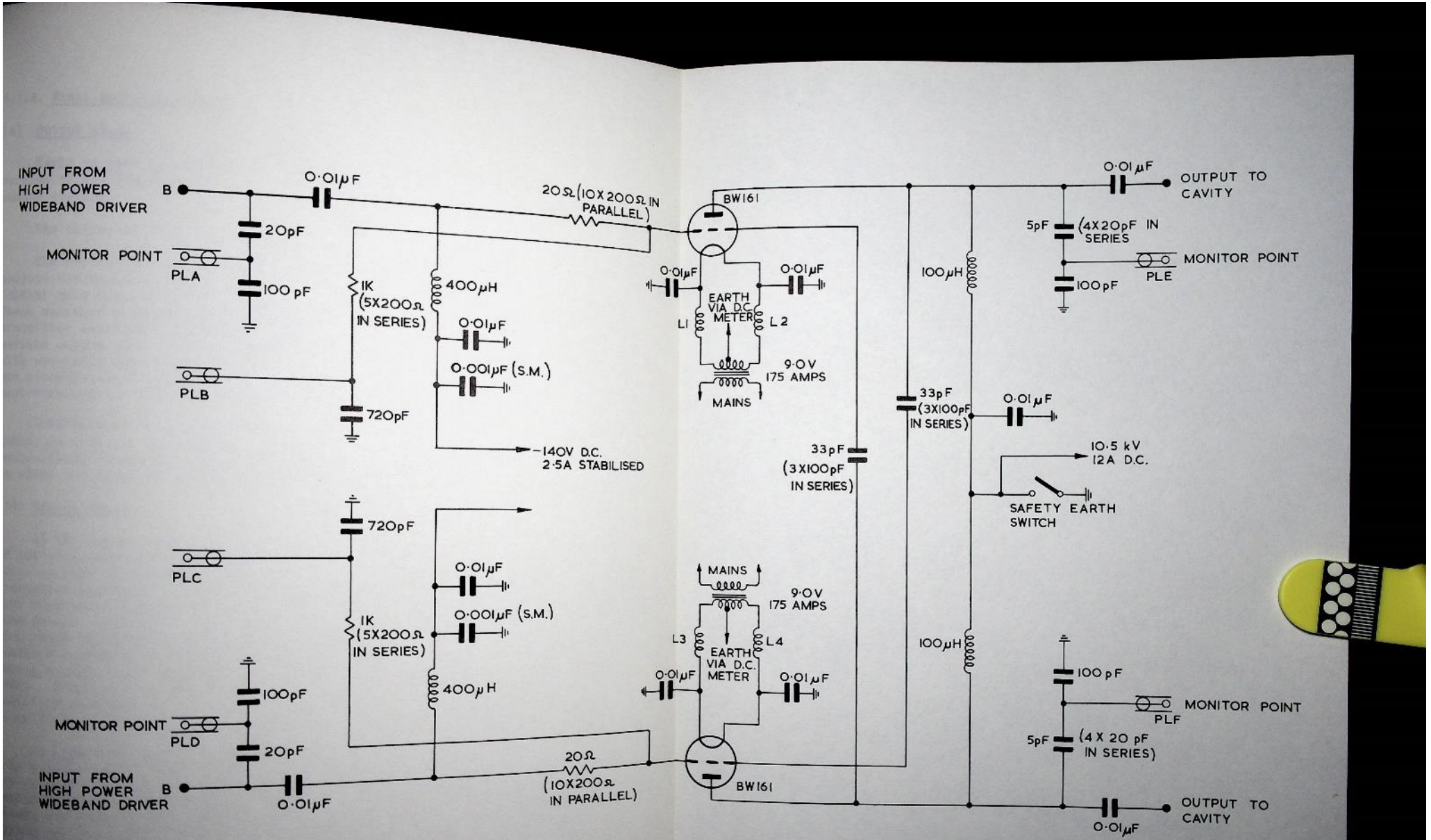

L1 – L4 ARE V.H.F. CHOKES.

Fig. 6.3.3(xiii) Prototype transmitter - Final stage power amplifier.

6.3.4. Final Amplifier Design

(a) Output stage

Early in 1960 it was necessary to consider production of a fully engineered version of the experimental transmitter capable of unattended operation from a remote station.

The choice of valve for the output stage was the BW 161.

The valves operate in conditions which utilise their characteristics to produce a transition from Class A to Class C as the drive signal is increased. Initial grid bias sets the quiescent anode currents at approximately 2 A each. These currents rise as the drive signal is increased but, due to the operating transition mentioned, are no more than 5 A when they are delivering the required maximum output power. The output stage is arranged as a wideband amplifier with aperiodic grid circuits and loosely coupled anode circuits, and the valves are cross-neutralised by variable vacuum capacitors. The basic circuit arrangement remained the same as that used for the experimental transmitter.

Neutralising the cold amplifier is achieved using a portable oscillator and detectors made for the purpose. A filter network is incorporated in the neutralising connection to prevent a self-oscillatory condition at the frequency at which the input of the cavity load shows a series resonance (about 18 Mc/s).

(b) Driver stage

At the higher frequency end of the band, the anode swing required from the BW 161's is increasing and under these conditions the reactive component of drive current is comparable with the peak electron grid current which has almost triangular waveform. A driver of the cathode follower type having low impedance, good regulation and the necessary bandwidth for the harmonic content was therefore considered. Various designs had previously been considered working in Class A with large standing valve currents. The driver circuit finally evolved is a combined push-pull phase-splitter/cathode follower. Type TY6/5000 W triodes having a high slope characteristic and consequently low cathode impedance are used. They operate with zero bias under quiescent conditions and with grid resistors returned to chassis. When driven, a transition from Class A to Class B operation takes place as increasing grid current develops grid bias.

At high input signal levels with the valves in Class B the driver produces only positive-going half cycle outputs from each cathode. Thus in any half cycle one cathode follower valve and one power amplifier are cut off. But the power amplifier tube is cut off by its steady d.c. bias voltage under a condition in which, due to push-pull coupling in the anode circuit, the anode potential is rising and this leads to an inefficient anode condition. The driver valves are therefore used additionally as phase splitters. Outputs are taken from resistance loaded anodes to the opposite grids by capacitors and the negative-going signals are used to swing the opposite valve into a true cut-off condition.

Under conditions of low signal input, this stage will operate in Class A to produce full waveform outputs in antiphase. D.C. returns to both grids and cathodes of this stage are made by a r.f. choke. The basic circuit is shown in Fig. 6.3.4(i).

(c) Low-power driver stage

To provide the required output of about 500 V peak from the cathode-follower phase-splitter stage an input of about 900 V peak is needed. To give this, the sub-driver has four radiation-cooled tetrodes (QY4/250) in parallel push-pull working in Class AB.

The interstage coupling has two elements: a shunt-fed transformer and a frequency compensating filter network. The transformer has very tightly coupled windings to transfer signals in push-pull to the input of the succeeding stage. The filter network can be described as having one and a half sections of a low pass, constant K filter with a mid-series termination which allows the input capacitance of the succeeding stage to be used as the mid-shunt capacitance. The stage is conventionally equipped with stopper resistances.

This sub-driver is itself driven by a cathode follower which has two radiation cooled triodes (Type TY3/250) in Class A push-pull. The output impedance of the stage matches the control grid requirement of the sub-driver amplifier. The r.f. input to the stage is fed via a full section, constant K filter network. The amplifier chain is completed by the five cascaded stages of the pre-amplifier.

The low-level r.f. excitation signal is fed into the first R.C. coupled single pentode stage together with the automatic level control signal which is applied to the high slope suppressor grid. Then follows a second R.C. coupled single pentode as a buffer amplifier. The next stage is a push-pull voltage amplifier, also used to provide unbalanced to balanced signal conversion, followed by an amplifier operated as a long-tailed pair and finally a Class A push-pull stage using two valves type QV06/20. These last two stages are also R.C. coupled but with some inductive compensation so as to utilise their high gain qualities.

The output of the tetrode (QV06/20) is about 180 V peak at an impedance level which matches the requirement of the cathode follower (TY3/250). Fig. 6.3.4(ii) shows the completed amplifier cubicle in position.

(d) Beam loading

The original r.f. specification included a maximum accelerated beam of 2×10^{12} protons per pulse. The power absorbed by the beam from the r.f. amplifier is proportional to frequency, and at 8 Mc/s is 1.6 kW for each 10^{12} p.p.p. From the actual performance of the amplifier at all frequencies, it is estimated that 5×10^{12} p.p.p. could be accelerated. The first limiting point is at 4.5 Mc/s where probably it would be dangerous to increase the phase angle.

6.3.5. Automatic Level Control of Gap Voltage

(a) Introduction

During the operating cycle, the amplitude of the accelerating voltage at the cavity gaps has to be controlled by a d.c. signal fed to the r.f. amplifier from an external source. This signal is derived from the same pick-up coil (placed in

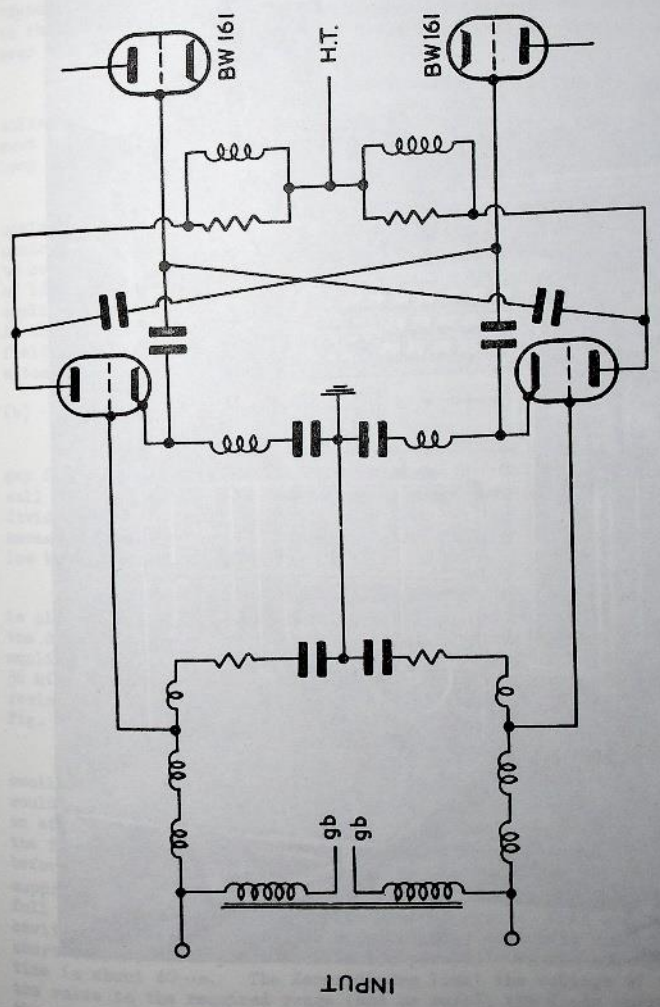

Fig. 6.3.4(i) Phase splitter/cathode follower driver circuit.

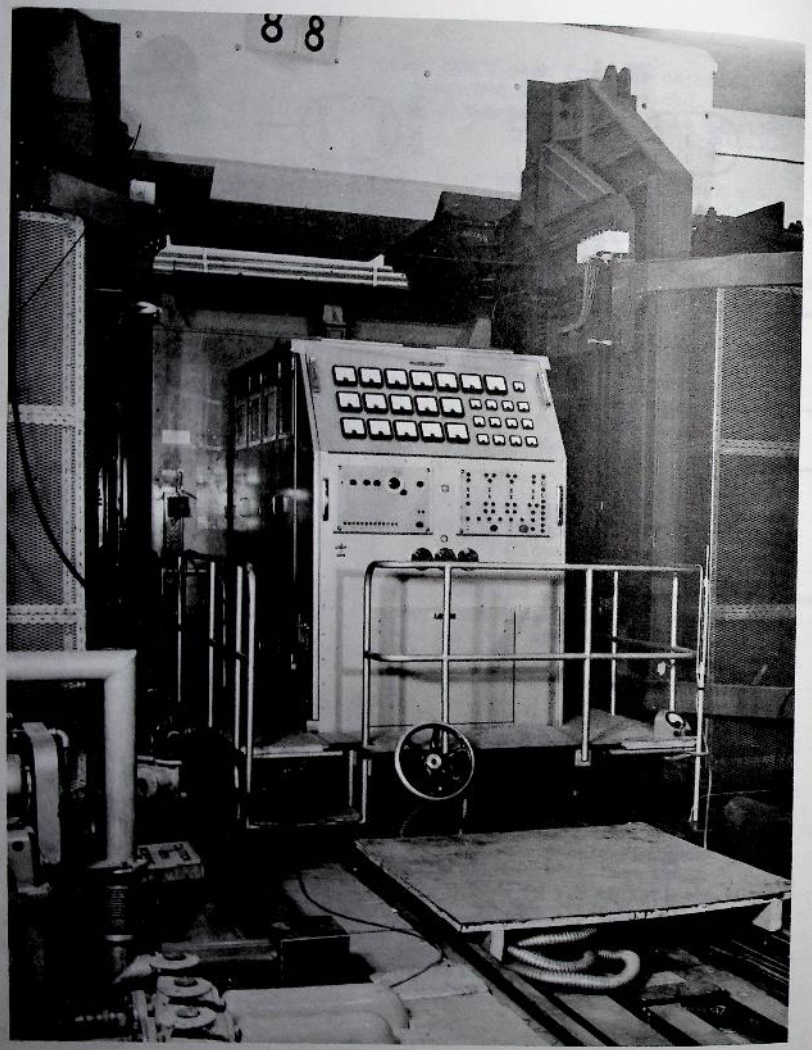

Fig. 6.3.4(ii) View of final amplifier cubicle in position.

the main magnet field) as that feeding the $\dot{B}$ signal to the P.F.G. and it is fed via a shaper to an emitter follower in the main control room. A control labelled "Synchronous Phase" feeds a pre-set proportion of this signal from the emitter follower to the r.f. amplifier. The cavity gap voltage must be proportional to this signal over a range extending down to at least one sixth of the full accelerating voltage.

A further requirement is that internally generated disturbances to the gap voltage such as those arising from ripple on H.T. supplies to the r.f. amplifier must be reduced to an acceptable level. These requirements are met in the closed loop circuit shown in Fig. 6.3.5(i).

A two-valve circuit is connected at the front end of the r.f. amplifier chain. The r.f. drive signal from the primary frequency generator is fed to the control grid of the first valve. The voltage on the suppressor grid is used to control the output from this stage. The gap voltage is reduced by a factor of 120 in a capacitance divider and rectified in a peak detector; this envelope is applied to the summing junction of a d.c. amplifier-cathode follower combination. At the summing junction it is compared with the programme voltage from the magnet field coil and the difference is amplified and fed to the suppressor grid of the automatic level control stage valve as a correction signal.

(b) Circuit details and performance

The amplitude sensing, capacitance potential divider is connected to the gap flanges of the drift-tube assembly and the output is fed through the cavity wall at a convenient point adjacent to the power amplifier. The cable from the divider must thread the ferrite core once on its way to the cavity wall and is necessarily rather long. Care is taken to damp any cable resonances which appear at low harmonics of any frequency within the band.

The detector uses germanium diodes in a simple voltage doubler circuit and is placed at the divider output terminal on the cavity itself. The output from the detector is fed via a 4.7 kΩ resistor to the summing junction of a d.c. amplifier which is followed by a cathode follower. A feedback resistor of value 56 kΩ is connected from output to input of this combination and across this resistor are connected Zener diodes and the series R-C combination shown in Fig. 6.3.5(i).

The series R-C combination serves to prevent the closed loop being self oscillatory in the frequency range in which its gain-phase shift characteristics would otherwise make it so. The combination is chosen not to have too adverse an effect on the transient response of the loop, which could be important under the following condition: if a signal exists on the gap voltage control terminal before the r.f. signal from the primary frequency generator is gated on, the suppressor grid of the first valve will be at approximately zero volts when the full r.f. signal is applied to its control grid. Full gap volts will appear in the cavity and these volts must be brought under automatic control in a time which is short compared with phase oscillation period. In the arrangement described this time is about 40 μs. The Zener diodes limit the voltage of the suppressor grid of the valve to the required range (and no more), the diode current being provided by the cathode follower.

In the normal mode of operation of the system the gap voltage control signal will be gated at a time which eliminates the over-shoot of gap voltage.

The gain of this d.c. amplifier network in the low audio frequency range is seen to be approximately 12. The gain at these frequencies, between the supressor grid of the first valve and the output of the detector, is approximately 13, and therefore the internally generated ripple voltages at these frequencies are reduced by a factor of about 150.

6.3.6. Phase Detector

(a) Principle

The basic principle is that of the conventional overlap phase detector, depending upon the production of rectangular current pulses, whose width depends upon the overlap between the positive half cycles of two input sine waves. These variable width pulses are then integrated to give a demodulated output. The two inputs are obtained, one from the grid of the final power amplifier valve via a 90° phase lag network (reference signal), and the other from the anode of the final valve via a 200:1 capacitive potential divider. Coincidence is measured using a 6BN6 gated beam valve so that when the power amplifier valve anode voltage is 180° out of phase with its grid, the grids of the 6BN6 are in quadrature, placing the phase detector at the centre of its range. If the valve anode is other than 180° out of phase with respect to the grid, then the 6BN6 grids will overlap to a greater or less extent.

Development of the phase detector has taken place in the three stages.

(b) First circuit

The final r.f. power amplifier stage is in push-pull and advantage was taken of this to employ two 6BN6's with paralleled outputs connected, as shown in Fig. 6.3.6(i)-(a), thus deriving two current pulses per r.f. cycle instead of one. This doubled the sensitivity.

Performance was satisfactory provided the r.f. amplifier operated at full gap voltage throughout the frequency band. However, the cavity is required to operate at a much lower gap voltage at injection, and choosing a figure of 1 kV from 1.4 Mc/s to 2.0 Mc/s, there is insufficient input at this level to the 6BN6's (particularly from the power amplifier grids). It was necessary to provide gain at the lower r.f. frequencies between the phase detector inputs and the 6BN6's. This was achieved by replacing the cathode followers with cathode coupled limiters (Fig. 6.3.6(i)-(b)).

(c) Second circuit

Identical limiters were used, the simplified circuit being given in Fig. 6.3.6(ii). The advantages of this circuit are:

(i) At high input levels, it functions as a symmetrical clipper and thus assists the 6BN6 in amplitude limiting;

(ii) At low levels, it functions as an amplifier, consisting of a cathode follower driving a grounded grid stage, so that the input impedance is high and the amplifier is stable without neutralising;

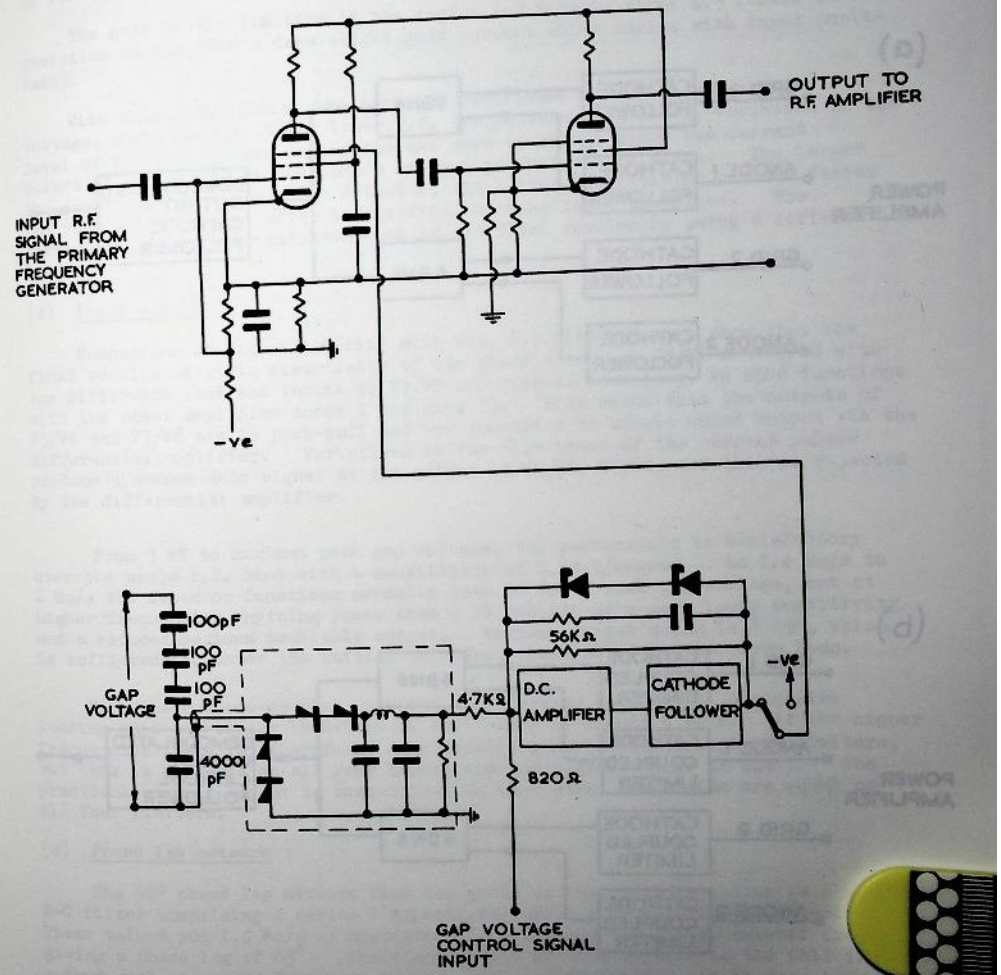

Fig. 6.3.5(i) Circuit for the automatic level control of gap voltage.

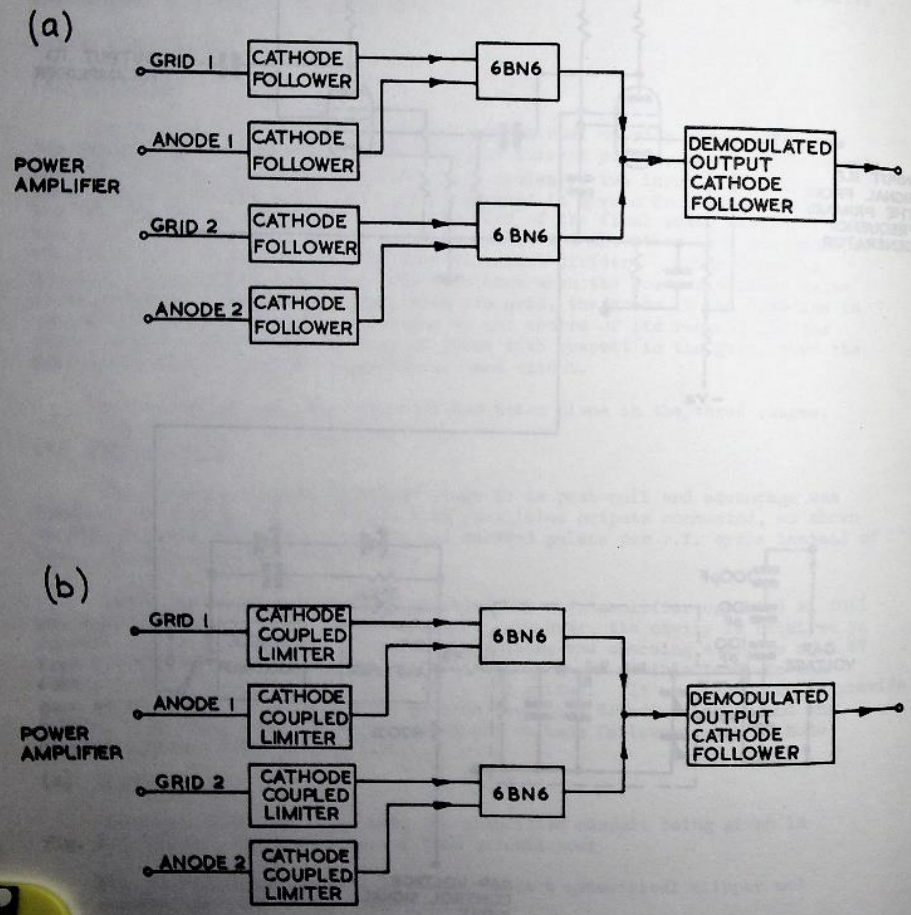

Fig. 6.3.6(i) Block diagrams of the first phase detector circuits.

(iii) Limiting is achieved by anode current cut-off on both half cycles of r.f. input (V1a then V1b) and, ideally, no grid current flows.

The gain of the limiters in the region 1-2 Mc/s is about 4.5 (there is some variation as the 6BN6's draw slight grid current which varies with input amplitude).

With this modification the detector functioned at a much lower gap voltage, particularly at the lower r.f. frequencies. However, variation in the level of the gap voltage caused the set zero to change since the current pulses at the anodes of the 6BN6's are not perfect square waves. The larger the input signal to the phase detector, the better the limiting and the faster the rise time, so that after integration the mean level increases. The difficulty has been largely overcome in the final version by using a differential system.

(d) Final circuit

Comparison of Fig. 6.3.6(iii) with Fig. 6.3.6(i)-(b) will show that the final version consists essentially of two phase detectors V5/V6 and V7/V8 with the difference that the inputs to V7/V8 are crossed over (e.g. V8 6BN6 functions with the power amplifier anode 1 and grid 2). This means that the outputs of V5/V6 and V7/V8 are in push-pull and are converted to single ended output via the differential amplifier. Variations in the rise times of the current pulses produce a common mode signal at the output of V5/V6, V7/V8, and this is rejected by the differential amplifier.

From 3 kV to maximum peak gap voltage, the performance is satisfactory over the whole r.f. band with a sensitivity of 0.55 V/degree. At 1.4 Mc/s to 2 Mc/s the detector functions normally down to 600 V peak gap voltage, but at higher frequencies anything lower than 3 kV results in a much lower sensitivity and a reduced maximum available output. Maximum output swing is $\pm$ 25°, which is sufficient to cover the initial transient phase error in the servo loop.

With the cathode-coupled limiters each feeding two 6BN6's, capacitive loading puts the linear bandwidth of the former at around 8 Mc/s. At the higher frequencies there is, therefore, considerable phase shift through the limiters, but this is balanced on all four inputs and the overall error is small. The practical circuit layout is symmetrical so that stray capacities are equal on all four limiters.

(e) Phase lag network

The 90° phase lag network from the grids of the power amplifier is a simple R-C filter comprising a series 1 kΩ resistor and a parallel 1200 pF capacitor. These values put 1.4 Mc/s at approximately ten times the filter cut-off frequency, giving a phase lag of 85°. One disadvantage of this network is the fall in output with increased frequency at the rate of 6 db/octave, but it does have the advantage that harmonics are attenuated, (2nd harmonic - 6db, 3rd harmonic - 9.5db). Second harmonic distortion of the type encountered in the grid waveform, after transmission through the network, would result in a waveform which is

symmetrical about the time axis, and has zero crossing points which are not displaced so that the phase detector functions correctly. The exaggerated waveforms shown in Fig. 6.3.6(iv) illustrate this point (the waveform (b) has been amplified x 10 for comparison).

Transmission time through such a network is not constant for all frequencies. The power amplifier grid waveform is however, fairly sinusoidal and there is no problem from the distortion point of view.

(f) Physical arrangement

The phase detector unit is mounted in the r.f. amplifier cubicle, and connected to the anode potential dividers and the grid lag networks with coaxial cables of length 5 ft and 7 ft respectively. At the sending end of these cables, resistors of value equal to the cable Z_o (100 Ω) have been inserted in series. On the assumption that the cables are lossless and terminated in an open circuit (a good approximation as the phase detector input impedance is high), it can be shown that the magnitude of the ratio of source voltage to received voltage at the detector is unity and independent of the line length. This reduces voltage variations that would occur due to transformation on the cables. Furthermore, viewed from the phase detector, the cables are approximately matched instead of presenting a high-Q circuit at the $\frac{\lambda}{4}$ resonant frequency of 24-30 Mc/s. The phase relationship between the source and the detector input now depends on line length as in a matched line ($\phi = \tan^{-1} \beta\ell$). The 2 ft difference in grid and anode leads contribute a maximum error of 5 degrees as the r.f. frequency changes but this is compensated for elsewhere.

(g) Semiconductor phase detector

Earlier in the development programme a transistorized phase detector was designed operating on the same principle of overlapping square waves. This showed promise when tested on the bench but difficulties arose in adapting the unit to the r.f. amplifier. The maximum input to the detector (determined by transistor base-emitter ratings) was around ± 0.5 V, and it was necessary to employ diode limiters on all inputs (Fig. 6.3.6(v)).

In this circuit the clipping and squaring of the waveform was performed at the outset before reaching the phase detector proper. Unsymmetrical clipping displaced the zero crossing points and the detector did not function correctly. Symmetrical clipping was difficult to achieve, due to variations in the detector input impedance as the input transistors were switched. There were also hole storage effects in the diodes. It was difficult to balance phase shifts through the diode limiters, as the input levels from the power amplifier varied over such a wide range.

Development was not pursued as the thermionic detector showed more promise, but it is not thought that a semiconductor phase detector is impossible, especially with improvements in modern transistors and diodes. Considerable work on the problem would be required, however, and the question of adequate cooling in the power amplifier cubicle would require special attention. Alternatively, to avoid damage by radiation, the phase detector would have to be located remotely, and long, matched cables would have to be used.

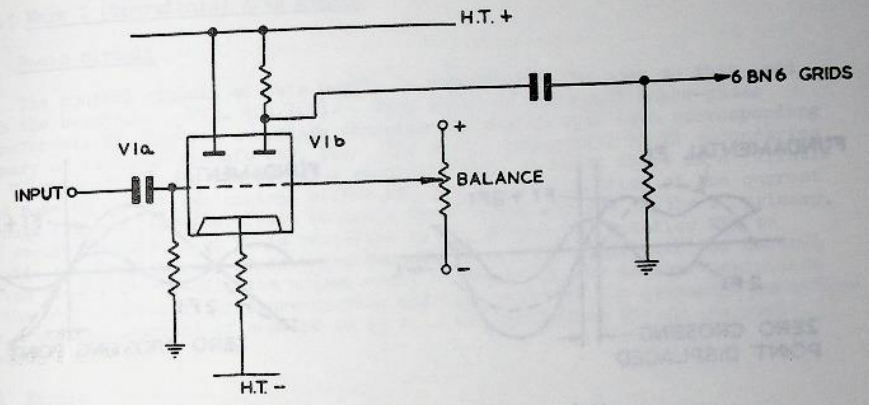

Fig. 6.3.6(ii) Second phase detector circuit.

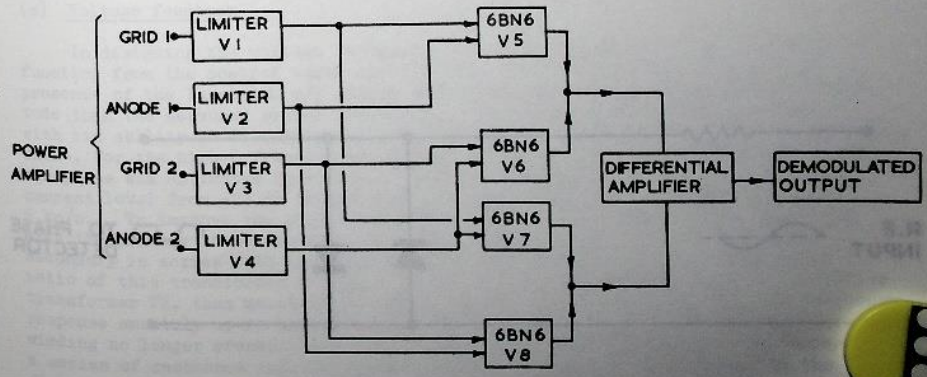

Fig. 6.3.6(iii) Block diagram of final phase detector circuit.

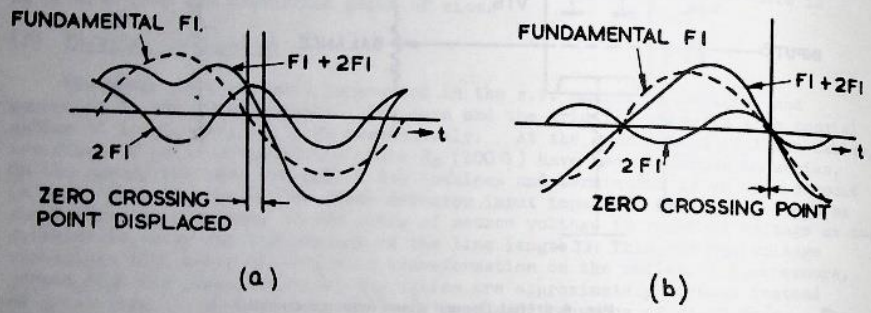

Fig. 6.3.6(iv) Waveforms transmitted through the phase lag network.

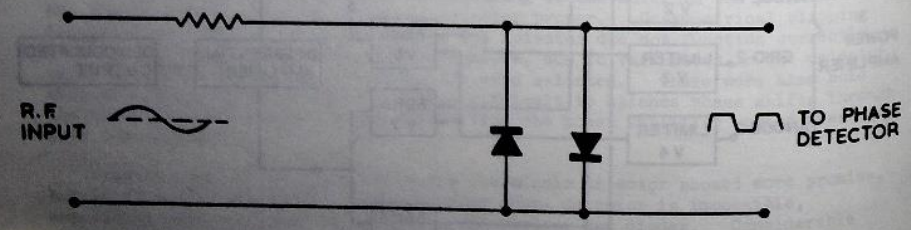

Fig. 6.3.6(v) Diode limiters on the semiconductor phase detector input.

6.3.7 Mark I (Thermionic) Bias Supply

(a) Basic circuit

The control circuit of this supply is essentially the same as that used with the Bevatron. Fig. 6.3.7(i). Each phase of the input three-phase transformer, T1, has its secondary connected in series with each corresponding primary of the load transformer, T2. The delta arrangement of T1 secondaries and T2 primaries feeds the selenium rectifier MR1, on which there is a variable load made up of the two control valves LV1 and LV2. Variation of the current through LV1 and LV2 effectively controls the voltage applied to the T2 primary. The secondary voltage of T2 is rectified by the germanium rectifier MR2 to provide the load current up to a maximum of 800 A. Ideally, with the control valves biased to cut-off, the output would be zero, but the inverse resistance of the selenium rectifier draws current and the output of the germanium rectifier has a standing current of some 10 to 15 A. This is backed off as described later.

(b) Ripple

The utilisation of a three-phase supply ensures that the ripple current in the output is small and is approximately 4% of the d.c. load current, though this percentage varies throughout the current range as the cavity inductance changes. Reduction of this ripple with a conventional smoothing circuit is not possible, for this would increase the bias supply time constant, but with the application of voltage feedback the current ripple has been reduced to less than 0.3% over the whole range. With the bias supply in the phase detector and cavity tuning loop, the phase modulation due to bias current ripple is never more than 1° peak in the r.f. frequency range 1.4 Mc/s to 2.0 Mc/s, and negligible over the remainder of the band.

(c) Voltage feedback

In designing the voltage feedback circuit, measurement of the transfer function from the control valve grids to the output was complicated by the presence of the large 300 c/s ripple component, which was far greater in amplitude than the measured signal frequency. The Resolved Component Indicator with its ability to discriminate, was used successfully for the lower frequencies, while, for the higher frequencies, a Wave Analyser gave the amplitude plot and and phase was estimated from this. The small signal d.c. gain varied with current level from -23 db to -36.5 db with a response flat to approximately 5 kc/s. To improve the high frequency response, a transformer was connected with the primary in series with the control valves anode circuit and the secondary in series with the output of the germanium rectifier. The turns ratio of this transformer is 200:1, which is the same as the germanium rectifier transformer T2, thus maintaining ampere-turns balance and extending the frequency response smoothly up to some 50 kc/s. Above this frequency the cavity bias winding no longer presents a simple inductance to the bias supply but enters a series of resonance and anti-resonance points, due (it is thought) to the distributed decoupling capacitors from the bias winding to the cavity skin forming, in effect, an artificial transmission line. The performance of the fast transformer is such that it will pass to the load all signal frequencies

above about 20 c/s, while signal frequencies below 20 c/s to d.c. reach the load via T2 and the germanium rectifier. As a result of the load inductance a rapid decrease of cavity current can demand a negative voltage swing, although the current will remain unidirectional. Without the fast transformer in circuit this is not possible as the germanium rectifier acts as a clamp to earth for negative potentials. The available negative swing however is limited, particularly at low current levels, where the control valves are biased towards cut-off.

The preamplifier preceding the control valves is a conventional d.c. amplifier consisting of two long tailed pairs and an output cathode follower. Overall voltage feedback is taken from the output of the cathode follower back to the first long tailed pair. The small signal d.c. gain is in the range +30 to +34 db, with a 3 db bandwidth at approximately 50 c/s. The response has been carefully tailored by networks in the feedback path to give a gradual fall of gain with a maximum phase shift of 60° in the region of 500 c/s and less at higher frequencies. Initially the peak in the closed loop response of this unit occurred close to 100 kc/s placing a high impedance in the grid circuit of the control valves at this frequency. With a 100 kc/s resonance in the anode circuit there was sufficient feedback for these valves to oscillate. The peak has now been reduced and moved to beyond 250 kc/s and the system is stable.

With the addition of a high gain operational d.c. amplifier, the voltage feedback loop is arranged as in Fig. 6.3.7(ii).

The d.c. gain of the d.c. amplifier is 60 dB with a bandwidth of 150 c/s and determines the d.c. drift of cavity voltage. This amplifier is a chopper stabilised type with a low drift figure. With the closed loop gain set at x 9, the long term drift in bias current is about 0.05 A, assuming a resistance of about 20 mΩ for cavity winding and leads. It is possible therefore, to set the initial cavity bias sufficiently accurately for the cavity to be less than one degree off tune at the commencement of the acceleration cycle (≙ 1.4 Mc/s). The backing off supply shown in Fig. 6.3.7(ii) enables the cavity current to be zero despite the standing current mentioned in 6.3.7(a). The standing current will equal the backing off supply current, whilst the voltage feedback maintains zero volts across the load for zero signal input. Adjustment of R now provides a means of setting the standing current to a value higher than the previous minimum and still maintaining zero current in the cavity. This is useful, as the control valves will now function with a higher initial bias and a reasonable quiescent current, so that the voltage feedback is fully operational. Drifts in the backing off currents are not important as they are automatically compensated for by the feedback loop.

The bandwidth of the supply with voltage feedback as above is 3 db down at 20 kc/s.

(d) Automatic cavity tuning

Fig. 6.3.7(iii) shows in simplified form the arrangement of the bias supply in the automatic cavity tuning loop. The auxiliary amplifier raises the d.c. loop gain by + 17 db and is tailored to stabilise the control loop consistent with the best frequency response. The auxiliary amplifier response can be approximated as shown in Fig. 6.3.7(iv). The complete closed loop frequency response varies with the bias current and is plotted against r.f. frequency in Fig. 6.3.7(v).

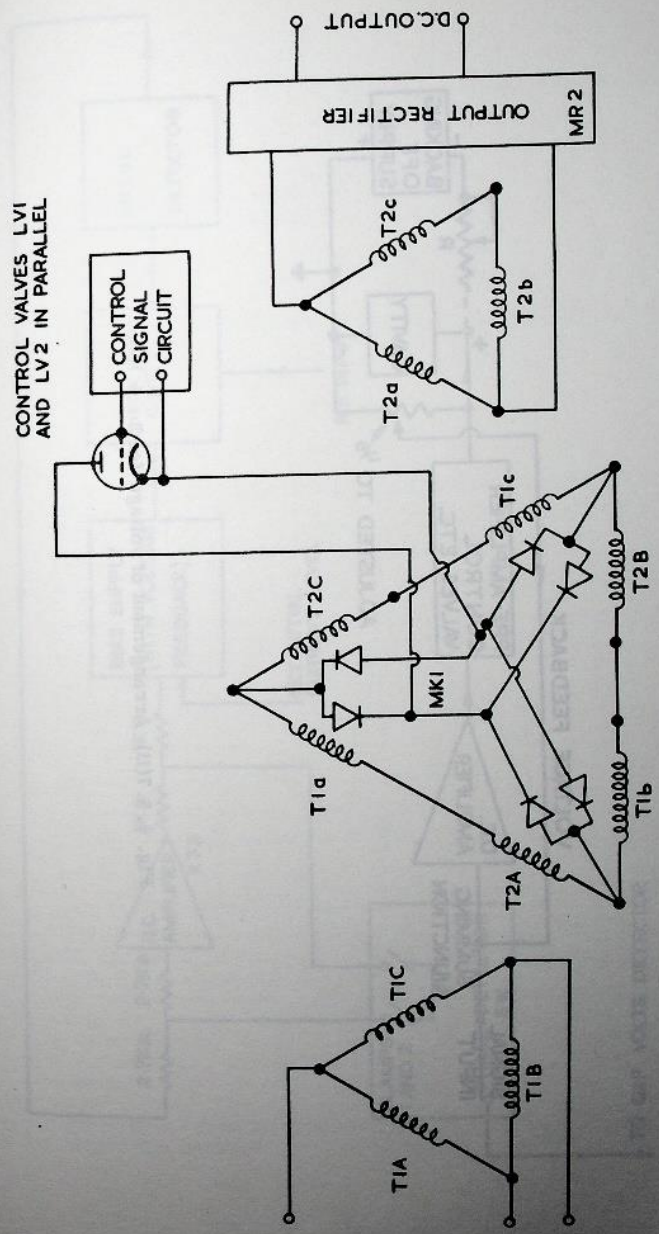

Fig. 6.3.7(i) Mark 1 thermionic bias supply circuit.

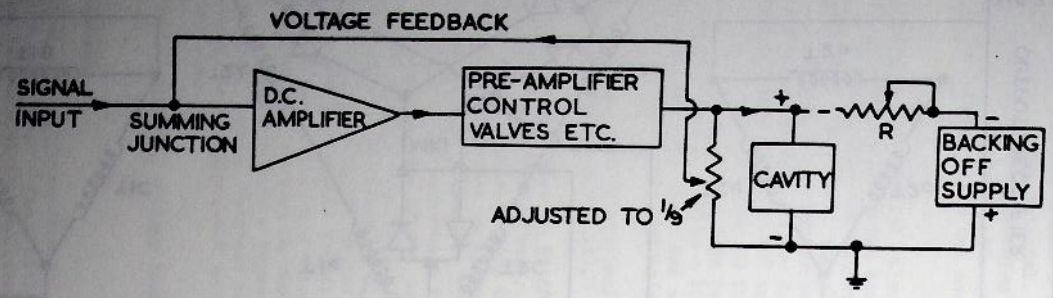

Fig. 6.3.7(ii) Arrangement of voltage feedback loop.

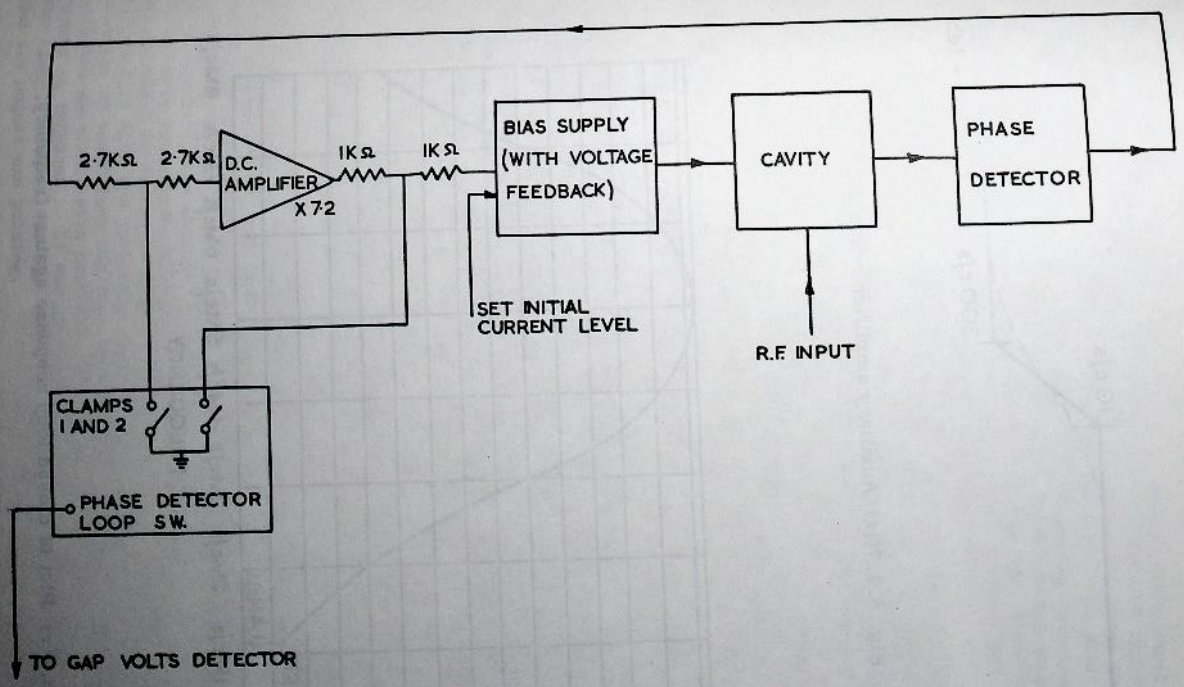

Fig. 6.3.7(iii) Arrangement of the bias supply in the automatic cavity tuning loop.

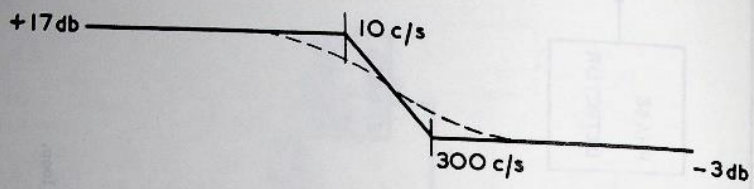

Fig. 6.3.7(iv) Auxiliary amplifier response.

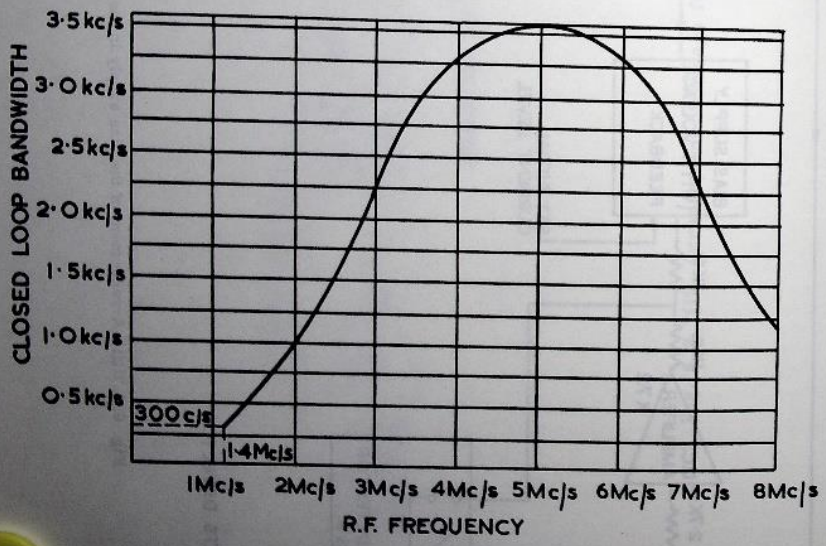

Fig. 6.3.7(v) Plot of closed loop response against frequency.

At the commencement of acceleration (≏ 1.4 Mc/s) the control loop frequency response is 300 c/s with an open loop d.c. gain of approximately 3000, these figures primarily determining the initial transient phase error which takes the form shown in Fig. 6.3.7(vi). After the transient, the phase error is negligible being less than 2° over the band (disregarding inaccuracies in the phase detector). In designing the servo loop, small signal measurements indicated the possibility of bandwidths greater than those achieved, but these were unobtainable in practice because of oscillation (at 1 kc/s) under large signal conditions, initiated by overloading at the higher signal frequencies.

Referring again to Fig. 6.3.7(iii), the inputs to the auxiliary amplifier and bias supply are clamped to earth in the absence of r.f. volts on the cavity gap. This ensures that the control loop is only closed when the cavity is on tune, and therefore, the error signal is within normal working limits. Under certain open loop conditions the output of the phase detector may be quite large and the use of two clamps following one another ensures that no residual input reaches the bias supply (this would modify the set initial current level). In preference to two clamps in series on the input to the bias supply, one is used on the input to the auxiliary amplifier to prevent saturation of this amplifier under open loop conditions, since recovery would then have a long time constant.

(e) General remarks

(i) Efforts to increase the complete control loop frequency response at the 1.4 Mc/s point (to reduce the transient error) are restricted by the variation in cavity time constant as the current increases. The time constant is progressively reduced as the current increases, the change being in the ratio of 32:1 over the band, which makes stabilization difficult. The application of current feedback to the bias supply would reduce the time constant but not necessarily the ratio. A further difficulty in achieving stability over the band is a change in the open loop gain of 14.5 db with variation in bias current. This is plotted against r.f. frequency (without auxiliary amplifier) in Fig. 6.3.7(vii).

The fall in gain of some 9 db between 2 Mc/s and 1.4 Mc/s (the graph of bias current against frequency has an inflection at this point) is unfortunate, as the highest d.c. gain is needed here.

(ii) Given normal conditions in the cavity, no great difficulty was experienced with r.f. interference in the bias supply. The d.c. amplifiers (particularly the voltage feedback amplifier with its high d.c. gain of x 1000) required the most attention, and it was necessary to prevent r.f. loop currents flowing through the signal earths. This has been achieved by grounding the signal earths to the chassis via capacitors, and increasing the impedance of the signal earth connections with r.f. chokes. Direct grounding of the signal earths, which is desirable from the r.f. point of view, was not possible due to difficulties with low frequency loop currents. To facilitate the isolation and reduction of earth loop currents, all co-axial leads have been terminated on insulated material, with provision for grounding or inserting resistance in the screens as required. It was noticeable that some differences in earth potentials (for example between the r.f. driver chain and bias supply) were only apparent when the magnet was pulsing.

(iii) Due to hole storage effects in the germanium rectifiers there are large voltage spikes on the bias supply output at 300 c/s repetition frequency. These spikes have a ringing frequency of approximately 100 kc/s and damp out in about 5 to 10 cycles. Spikes of approximately 1-2 degrees of phase modulation are also visible on the output of the phase detector. The practice of employing hole storage capacitors across the T2 secondary has not been employed, as it is preferable to retain the high ringing frequency of short duration.

(iv) The voltage needed across the bias winding is dependent chiefly on dI/dt rather than I, and it is not therefore possible to protect the supply against current overload by limiting the voltage in any way. Current limiting must be achieved by monitoring the actual bias current, and originally the voltage drop across a resistor in series with the cavity was used for this purpose. However, the current required has increased to a level (800 A) where load resistance has to be reduced to a minimum, and this monitoring resistance has had to be dispensed with. An alternative solution is being sought.

(v) Referring to the transfer function of control valve grids to the output, there is considerable attenuation at 300 c/s and higher frequencies, which implies a large 300 c/s ripple component on the grids of these valves. At mean grid levels of approximately -10 V the superimposed component of ripple is just swinging into grid current. Any increase of mean level over -10 V, limits the voltage feedback loop gain and the ripple component is no longer "bucked out". Similarly with the higher signal frequencies, the limit is set by the onset of grid current and is the overloading referred to in 6.3.7(d). Once overloading does occur, the onset of distortion is sudden and drastic as a consequence of the voltage feedback.

The transfer function also shows that at the higher current levels the d.c. gain from control grids to output is approximately x 0.06. At a given output current, a small change in load resistance will demand a change in grid voltage 17 times that of the output voltage. For example, assume the current is 800 A, then a 2 m Ω increase in load resistance will require 1.6 V rise at the output, and this in turn requires an increment at the control grids of 1.6 x 17 = 27 V. The Mark I supply is therefore very dependent on keeping load resistance to a minimum at these high current levels.

(vi) The present transient phase error is considered satisfactory but if it should prove unacceptable in the future, there is the possibility of programming the bias supply over the first 2 ms or so of the frequency sweep. This could be achieved by injecting a suitable waveform into the summing junction of d.c. amplifier No. 2.

6.3.8. Mark II (Transistorised) Bias Supply

(a) Purpose

The Mk II bias supply was developed to provide a more flexible means of automatically tuning the r.f. cavity with a better overall performance.

It was designed:-

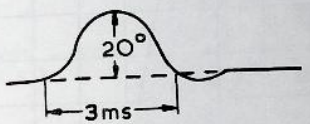

Fig. 6.3.7(vi) Initial transient phase error.

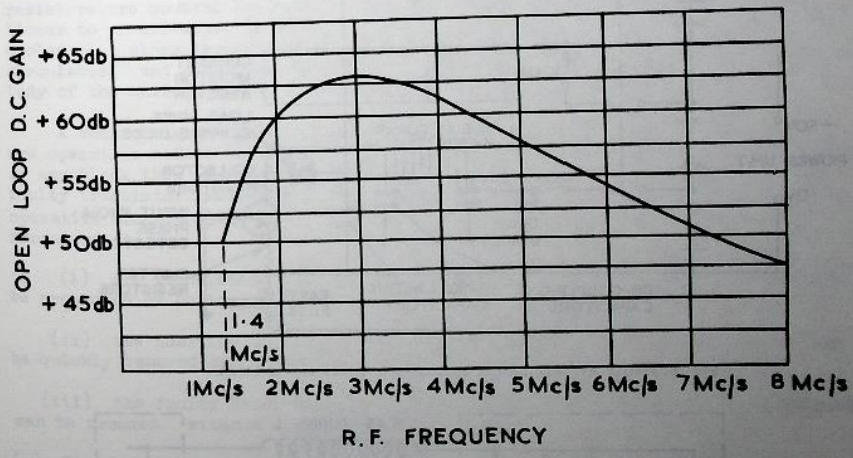

Fig. 6.3.7(vii) Plot of open loop d.c. gain against r.f. frequency

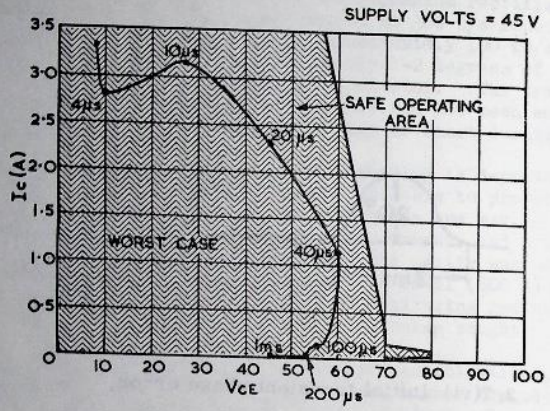

Fig. 6.3.8(i) Transistor voltage-current locus at turn off.

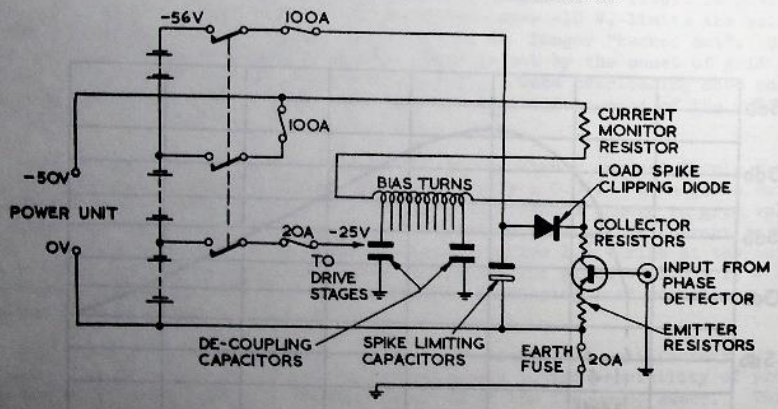

Fig. 6.3.8(ii) Arrangement of control unit, power unit and load.

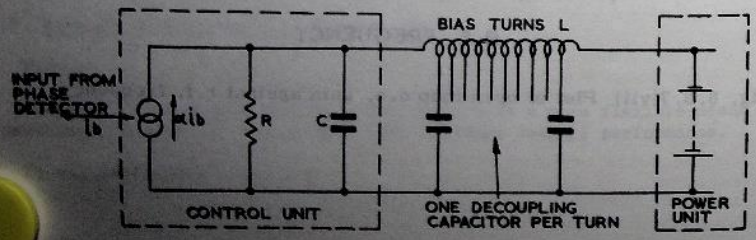

Fig. 6.3.8(iii) Simplified equivalent circuit of phase loop.

(i) to provide accurate phase control of the cavity r.f. voltage over the frequency sweep period,

(ii) to permit phase modulation of the cavity r.f. in the 2 to 5 kc/s (i.e. the synchrotron oscillation) band,

(iii) to deliver if required an increased current to the bias turns in the r.f. cavity.

The supply comprises a direct current power unit capable of delivering up to 900 A at 50 V via a control unit to the bias turns.

(b) Control unit

The control unit dissipates most of the output from the power unit. It consists of a parallel array of 192 power transistors divided into 8 distinct blocks, each operating with emitter and collector load resistors. There are subsidiary circuits, including drive stages, fault protection and fault readout circuits associated with each block. Under conditions of maximum power the emitter load resistors, collector load resistors, and power transistors dissipate 11, 18 and 10 kW respectively. Several cooling systems are employed in the control unit to remove the dissipated power: theemitter and collector resistors are mounted in ducts through which air is forced by a radial flow blower to an air-water heat exchanger; the transistors are mounted on water cooled heat sinks through which chilled demineralised water continuously circulates; and a smaller axial-flow fan ensures air flow through the main body of the unit to remove power dissipated in the drive stages.

A comprehensive system of interlocks ensures that all cooling systems are operative before the load is switched on. If a transistor breakdown occurs in any block, this is detected, the block is isolated and the position of the faulty transistor indicated. The control unit may then be used with 7 blocks operative and can carry up to two faulty blocks. If a fault occurs it is necessary that:-

(i) all transistors in the block containing the faulty transistor should be protected by bottoming,

(ii) the position of the failed transistor should be displayed so it can be quickly removed and replaced,

(iii) the faulty block should be disconnected automatically so that operation can be resumed without a complete shutdown.

(c) Choice of transistors

The important transistor ratings are:-

(i) Maximum collector emitter voltage ($V_{ce\ max.}$) (i.e. with base and emitter shorted). This was compared with a careful assessment of the collector voltage under all transient conditions. Since the load is inductive, the most severe conditions occur at turn off on full load, especially when turn off time

is rapid (100 μs or less). Charts of maximum reliability area, available from the transistor manufacturers, are most useful in assessing the operating conditions. Fig. 6.3.8(i) shows the voltage-current locus for a single power transistor during the first millisecond of turn off from full load.

(ii) Maximum power and junction temperature. To ensure good reliability the junction temperature in the output transistors is kept low. The transistor finally chosen is rated at 150 W and 100°C. The actual maximum power per transistor under fixed frequency conditions is 70 W, a requirement to be met occasionally during tests. Under these conditions the junction temperature does not exceed 60°C.

(iii) Cutoff frequency in common emitter circuits. This was specified at 10 kc/s or above to meet the phase modulation requirement.

(d) Power units

The possibility of power transistor breakdown, due to mains surges, rectification spikes and the stored energy associated with the inductive load, placed a special requirement on the power supply. The margin between E_{Δ} (the nominal output voltage at 50 V d.c.) and V_{ce} max. (80 V) requires good smoothing to reduce rectification spikes and ripple to a tolerable level. The energy stored in the bias turns at full load is about 60 J, this must be safely absorbed by the power supply also. The following possibilities, all employing 3 phase transformer/rectifier sets as the basic system, were considered:-

(i) Output regulation by means of series transductors in the primary side was rejected because it was felt it offered insufficient protection.

(ii) Regulation by means of silicon controlled rectifiers (S.C.R's) was also rejected for the same reason.

(iii) Series regulation by motor-driven Brentford regulator - fast transients being absorbed by a heavy duty lead acid battery floated across the output. This was chosen as the most simple and reliable arrangement providing continuous protection, although it is somewhat bulky.

(iv) As (iii) but with a nickel cadmium battery of compact sintered block construction - heavy current access to the battery taking place via S.C.R's only when surges occur and when the load energy is delivered at the completion of each sweep.

This was rejected because of its greater complexity though it is considered it would work effectively and be more compact than (iii).

A skeleton circuit showing the arrangement of power unit, control unit and transistors is shown in Fig. 6.3.8(ii). The capacitors are high current heavy duty electrolytics for reducing very fast spikes at the transistor collectors (where these are of order tens of microseconds, battery inductance becomes a considerable factor). It is important that they and the spike clipping rectifiers be placed as close as possible to the control unit terminals.

(e) Battery fuses and earth fuse

For safety reasons the battery is fitted with isolator and fuses. Standard H.R.C. fuses at 100 A were chosen to compromise between low resistance and low fusing current.

A low current fuse provided between +50 V and earth, which is essential for safety reasons, developed unwanted feedback voltages in series with the input signal path. It was necessary to separate signal and earth return paths to avoid unstable modes in the phase and current feedback loops.

(f) Phase and current feedback loops

The control of phase or current are alternatives determined by the conditions required at the start of the frequency sweep. At the end of injection, a few hundred microseconds may elapse before the full voltage is applied to the r.f. cavity. During this interval, the current control loop is designed to maintain bias current at the right value, rising at the correct rate to ensure that phase errors are minimised in the cavity and r.f. drive chain. At the instant full volts are applied to the cavity, the bias loop is automatically switched to phase control and remains so until the completion of the sweep. The current reference may be derived from an independent source or from the integrated B signal derived from the magnet.

Because the bandwidth requirement of the current loop is not stringent, stabilisation is not difficult. The phase loop presents a more serious problem. The basic open loop transfer function of the phase loop is of the form:

$$\frac{1}{LC\,S^2 + \frac{L}{R}S + 1} \times \frac{1}{S + 2\pi f_{\alpha}}$$

with an equivalent circuit as shown in Fig. 6.3.8(iii).

		No Load	Full Load
L =	bias turns inductance	5 mH.	0.13 mH
C =	combined depletion layer capacitance of the power transistors	1.42 μF	7.2 μF
R =	total parallel output resistance of the power transistors	12.5 Ω	1.46 Ω
f_{α} =	cutoff frequency of the power transistors	100 kc/s	25 kc/s

The three principle elements form an overdamped LCR circuit:

		No Load	Full Load
Natural frequency $f_n = \frac{1}{2\pi\sqrt{LC}}$	=	1.9 kc/s	5.3 kc/s
Damping factor $D = \frac{1}{2R}\sqrt{\frac{L}{C}}$	=	2.4	1.5

The variation of f_n from no load to full load is not great because as the bias turns inductance falls with increasing load current, the capacitance associated with the transistors increases. Also the resistive component of the output impedance falls, so that D does not vary greatly. The actual situation is altered by the presence of 0.1 μF r.f. decoupling capacitors between the bias turns and earth. Their effect is to make the bias winding look like a transmission line with a large propagation constant. The open loop phase-frequency responses show phase lags in excess of those associated with the simple circuit of Fig. 6.3.8(iii).

In order to provide the bandwidth necessary for beam control purposes, series stabilisation was chosen to compensate for the considerable lags in the bias turns. The limitations on such methods arise from noise and other unwanted signals in the error signal path. By keeping ripple and other forms of interference low in the bias loop, closed loop bandwidths of order 10 to 15 kc/s have been obtained.

The equipment was fully tested under pulsed and swept frequency r.f. conditions.

6.3.9 General Arrangement of High Power R.F. System

(a) Layout of equipment in magnet room

In the normal working position the cavity is located in straight section 8 and the power amplifier immediately adjacent to it on the inside of the magnet ring (Fig. 6.3.9). The cavity and amplifier are both mounted on wheels and run on radial rails on the floor of the magnet room. To examine the cavity, it can be detached from the amplifier and rolled towards the outside of the ring; for r.f. test purposes, both amplifier and cavity can be withdrawn towards the centre of the ring. All electrical connections to the cavity and amplifier are made by flying leads to junction boxes on the floor and these junction boxes are paralleled to extension boxes near the centre of the ring for use when the cavity and amplifier are in the test position. The level control and phase detector circuits and their power supplies are situated inside the amplifier cubicle.

The thermionic bias supply sits on the magnet room floor a little way from the straight section. The transistor bias supply, because of its sensitivity to radiation damage, is located in a cellar below the ring close to the r.f. straight section. It is hoped that the transistor bias supply will have the better performance and be normally used, but the thermionic bias supply is being retained for some time as a spare and the connections can easily be interchanged.

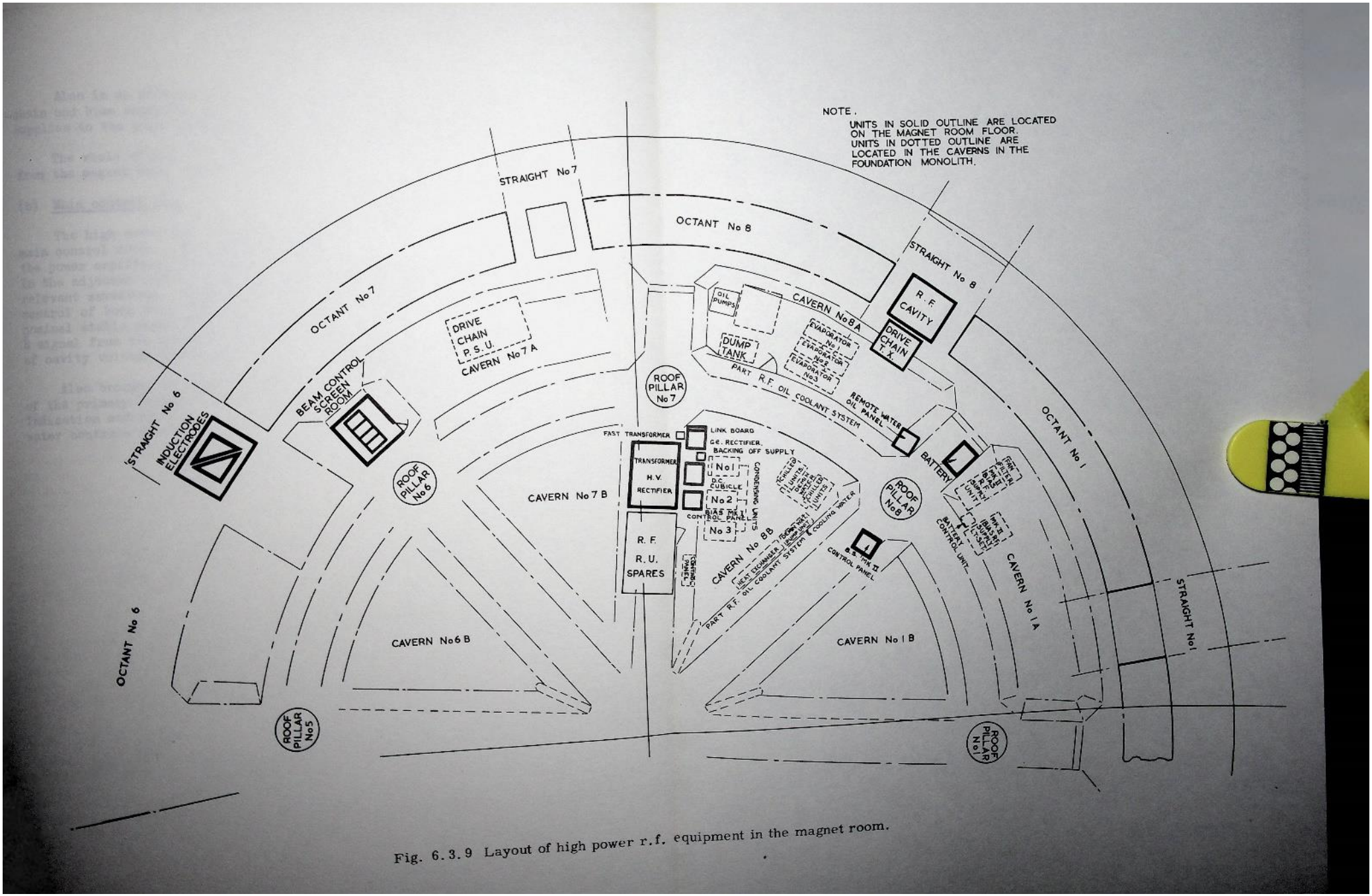

Fig. 6.3.9 Layout of high power r.f. equipment in the magnet room.

Also in an adjacent cellar are the water cooling plant for the r.f. drive chain and bias supplies, the oil chilling plant for the cavity, and the d.c. power supplies to the power amplifier.

The whole of the r.f. system including water and oil plant can be operated from the magnet room floor.

(b) Main control room

The high power r.f. equipment is controlled from two 6 ft racks in the main control room. One rack holds the remote indication and controls for the power amplifier, and remote indication and control of the oil chilling unit. In the adjacent rack is an oscilloscope and a patch panel for monitoring of all relevant waveforms. Also in this rack are panels for metering indication and control of both bias supplies. A further panel provides adjustment of the nominal stable phase angle by altering the gain of an amplifier which feeds the B signal from the primary frequency generator to the power amplifier for control of cavity voltage amplitude.

Also brought to these racks are an indication of the correct functioning of the primary frequency generator and some monitor points from that equipment. Indication and control of the cooling water is incorporated in the overall water controls panel for the machine.

REFERENCES FOR SECTION 6

1. D. J. Thompson. Notes on a drift tube cavity for a proton synchrotron. Internal report HAG/RF/1.

2. D. J. Thompson. Ferrite for the accelerating cavity of Nimrod; its electrical properties and their measurement. NIRL/R/5.

3. P. D. Dunn, S. M. Third and D. J. Thompson. The electrical characteristics of the r.f. accelerating cavity for the 7 GeV proton synchrotron. Internal report HAG/RF/8.

4. F. E. Terman. Calculation of Class C power amplifier performance. Radio Engineers' Handbook, Section 5, page 444.

5. L. J. C. Appleby, R. C. Hazell, R. Kur and P. Wilde. The performance of an injection trigger pulse generator. NIRL/M/22.

SECTION 7

EXTRACTION SYSTEMS AND INTERNAL TARGETS

7.1. Slow Extraction System

7.1.1. Principles of Operation

(a) Review

The aim of the proton extraction system is to produce an external beam which contains an appreciable fraction of the accelerated protons and which can be focused with quadrupole lenses to a small image at a target. Small images are particularly necessary when using electrostatic separators in the secondary particle beam.

The basis of the system is that used on the Cosmotron (1,2). A target of a light material is used and the beam is moved towards the target to strike the "lip" (3) - a thin piece of the target standing proud of the main body. This lip reduces the amplitude of the radial betatron oscillations, reduces the energy spread of protons entering the target and also ensures that they traverse the whole target. The energy loss produced by ionization in the target causes the proton to take a new path, oscillating now about a mean orbit which is at a smaller radius than the target. Approximately at the innermost part of their oscillating path, the protons pass through the aperture of a magnet whose field deflects them outwards again. The deflection given is sufficiently large for the protons to travel right across the aperture of the machine and emerge as an extracted beam.

In emerging from the main magnet the protons have to pass through the fringe field which is defocusing in the radial direction and causes the beam to diverge. In the "Cosmotron" this divergence is counteracted by "extraction shims" attached to the outside of the magnet which reshape the fringe field in the region of the beam.

Preliminary calculations revealed that on Nimrod such a system would result in a beam which was too large to be accommodated by standard quadrupoles (mainly because of the larger machine radius) and also that it would be difficult to ensure good enough beam optics in the fringe region (even using special lenses) to allow the beam to be focused to a reasonable spot in the horizontal direction.

The first modification investigated consisted of incorporating a field gradient which was radially focusing in the deflecting magnet. (This was independently suggested by Gan'zhin (4)). This improved the beam considerably but not as much as was desirable. The beam at the magnet M (see Fig. 7.1.1(i) is spread out due to the variation of energy loss in the target (5) and is diverging due to the scattering of the protons in the Coloumb fields of the nuclei in the target (6) (the target is imaged at the extractor magnet). Hence while a focusing magnet can improve the situation with regard to the first effect it is unable to affect the second. A compromise by placing the magnet at a different position is not significantly better than the placing shown in Fig. 7.1.1(i).

(b) The Nimrod System

In the system designed for Nimrod (6) an additional element, a radially